

ARL-STRUC-R-444

AR-006-626

2

**AD-A242 972**



**DTIC**  
**ELECTE**  
**DEC 6 1991**  
**S C D**

**DEPARTMENT OF DEFENCE**

**DEFENCE SCIENCE AND TECHNOLOGY ORGANISATION**

**AERONAUTICAL RESEARCH LABORATORY**

**MELBOURNE, VICTORIA**

**Aircraft Structures Report 444**

**CRITICAL APPRAISAL OF THE McDONNELL DOUGLAS  
CLOSURE MODEL FOR PREDICTING  
FATIGUE CRACK GROWTH**

by

**M.J. BOS**

**91-17084**



Approved for public release

**REPRODUCED FROM  
BEST AVAILABLE COPY**

© COMMONWEALTH OF AUSTRALIA 1991

SEPTEMBER 1991

**This work is copyright. Apart from any fair dealing for the purpose of study, research, criticism or review, as permitted under the Copyright Act, no part may be reproduced by any process without written permission. Copyright is the responsibility of the Director Publishing and Marketing, AGPS. Enquiries should be directed to the Manager, AGPS Press, Australian Government Publishing Service, GPO Box 84, CANBERRA ACT 2601.**

**DEPARTMENT OF DEFENCE  
DEFENCE SCIENCE AND TECHNOLOGY ORGANISATION  
AERONAUTICAL RESEARCH LABORATORY**

Aircraft Structures Report 444

**CRITICAL APPRAISAL OF THE McDONNELL DOUGLAS  
CLOSURE MODEL FOR PREDICTING  
FATIGUE CRACK GROWTH**

by

M.J. BOS

**SUMMARY**

*The McDonnell Douglas fatigue crack growth model CNTKM8 has been used to predict crack growth in CCT-specimens with through cracks under four different load sequences, including a flight-by-flight sequence, and two stress levels. The predictions were compared against experimental data. The results ranged from fairly good for the more-structured sequences, to rather poor for the more-random sequences. Furthermore, the experimental trend of the structured sequences giving longer crack growth lives than the random sequences was not predicted correctly. An enhanced model was proposed, which was also tested. The predictions of this model were more consistent with the experimental data, and the above-mentioned experimental trend was also predicted correctly.*

*This report contains a detailed description of both models, including the equations that are relevant for the case of a CCT-specimen with a through crack, and of the tests that they were subjected to.*



© COMMONWEALTH OF AUSTRALIA 1991

---

**POSTAL ADDRESS:** Director, Aeronautical Research Laboratory  
506 Lorimer Street, Fishermens Bend 3207  
Victoria Australia

# CONTENTS

**SUMMARY**

**CONTENTS**

**NOTATION**

1. INTRODUCTION.....	1
2. THE MCAIR MODEL.....	1
2.1 Assumptions.....	2
2.2 Constant Amplitude Loading.....	2
2.3 Variable Amplitude Loading.....	4
2.3.1 Definition of Overload and Underload.....	5
2.3.2 Thickness Effect.....	6
2.3.3 Examples.....	8
3. ASSESSMENT OF THE MCAIR MODEL.....	9
3.1 Experiments.....	9
3.2 Constant Amplitude Data.....	9
3.3 Predictions.....	10
3.4 Thickness Effect.....	12
3.5 Discussion.....	13
4. ENHANCED CRACK CLOSURE MODEL.....	14
4.1 Actual Model.....	14
4.1.1 Constant Amplitude Loading.....	15
4.1.2 Variable Amplitude Loading.....	16
4.2 Predictions.....	18
4.3 Discussion.....	19
5. CONCLUSIONS.....	20
REFERENCES.....	22

**TABLES**

**FIGURES**

APPENDIX A COMPUTER PROGRAM CNT8SHR

APPENDIX B COMPUTER PROGRAM ARLECC

Accession For	
NTIS GRA&I	<input checked="" type="checkbox"/>
DTIC TAB	<input type="checkbox"/>
Unannounced	<input type="checkbox"/>
Justification	
By.....	
Distribution/	
Availability Codes	
Dist	Avail and/or Special
A-1	



## NOTATION

The following list of symbols is used throughout this report. Where possible the usual notation as found in the international literature has been sustained. Since most of the equations have been obtained from the listing of the computer program that incorporates the McAir model [6], however, it sometimes was more convenient to use that notation.

$a$	half crack length in centre-cracked tension specimen
$a_{ol}$	half crack length at time of overload
check	parameter that is used in test to decide whether $K_{max,ol}$ should be updated
$da/dN$	crack growth rate
effkr	proportion of opening stress to overload in overload cycle for $R = 0$
fr	ratio between cyclic and monotonic yield stress
$K_c$	fracture toughness
$K_{max}$	crack tip stress intensity based on maximum cyclic stress
$K_{max,eff}$	effective value for $K_{max}$
$K_{max,ol}$	crack tip stress intensity based on overload (= $K_{max}$ for CA-loading)
$K_{min}$	crack tip stress intensity based on minimum cyclic stress
$K_{min,eff}$	crack tip stress intensity based on opening stress in cycle
$K_{min,ol}$	crack tip stress intensity based on underload (= $K_{min}$ for CA-loading)
$N_d$	crack growth delay (in cycles) after a single overload
$R$	stress ratio, such as minimum over maximum stress in any cycle, though denoted as $K_{min,ol}/K_{max,ol}$ in McAir model
$w_{ol}$	size of plastic zone due to overload
$x_\alpha$	factor that accounts for material thickness in calculation of $K_{min,eff}$
$x_{fr}$	factor that accounts for cyclic material behaviour in calculation of $K_{min,eff}$
$x_r$	factor that relates $K_{min,eff}$ to stress ratio $R$
$\alpha$	retardation parameter, theoretically representing material thickness; in practice used to tune the crack growth model
$\beta$	equal to $(\alpha + 1)/2$
$\Delta K$	stress intensity range ( $K_{max} - K_{min}$ )
$\Delta K_{eff}$	effective stress intensity range ( $K_{max} - K_{min,eff}$ )
$\sigma_{max}$	maximum cyclic stress
$\sigma_{max,ol}$	maximum stress in overload cycle
$\sigma_{y,eff}$	effective monotonic yield stress, used in calculation of $w_{ol}$ to cover large scale yielding of net section

---

## 1. INTRODUCTION

The application of crack growth predictions has been highly stimulated by the current airworthiness requirements imposed by civil and military agencies. These requirements were initiated to ensure the fatigue safety and durability of a fleet of aircraft. Small cracks, either pre-existing at the time of manufacture or created by in-service conditions, are assumed to grow during the life of the aircraft. The growth of the crack should be predictable to provide guidance for inspection programs, which ensure that cracks will never propagate to failure prior to detection. For this purpose many crack growth models have been devised during the last three decades. None of these models is universally accepted however.

Finney and Machin [1] have examined four well-known load-sequence-effect models, Wheeler, Willenborg, Modified Willenborg and a Crack Closure model, for their effectiveness in predicting fatigue crack growth. Predictions from the models were compared against experimental crack growth data obtained using several reconstitutions of a range-pair counted flight-by-flight fighter load sequence. Although the Wheeler model gave reasonable results, none of the models correctly predicted the trends in experimental crack growth among the various reconstituted sequences.

This present work describes the assessment of a fifth crack growth model, viz. the McDonnell Douglas Contact Stress Model ('McAir model'). Essentially this model is based on the phenomenon of crack closure at positive stress levels. Again the above mentioned variations on a fighter load sequence have been used to estimate the accuracy of this model. The computer program that incorporates the McAir model is fairly extensive and offers several stress intensity factor solutions and other options such as: surface flaw, bearing stress correction for a crack at a hole and cracks with a residual stress intensity adjustment [2]. Only the basic option of a through crack in a centre cracked specimen is examined in this report.

## 2. THE MCAIR MODEL

The McAir crack growth model is based on crack closure, although it is classified as a contact stress model by the authors. It has been observed by Elber [3] and many others that fatigue cracks become physically closed during unloading at positive stress levels. During subsequent uploading the fatigue cracks are only opened if the load is sufficiently high. This can be explained with the effect of residual plasticity that is left in the wake of the crack tip as the crack grows through prior plastic zones. A method has been developed by Dill and Saff [4,5] to determine the displacements and the plastic deformations along the crack surfaces. In this way they were able to calculate crack closure under constant amplitude loading as a function of the stress ratio. In the McAir model this curve is

manipulated to obtain the minimum effective stress intensity factor, or opening stress intensity, for each block of cycles of a variable amplitude load sequence. It is assumed then that the same effective stress intensity range  $\Delta K_{\text{eff}}$ , defined as the maximum stress intensity  $K_{\text{max}}$  minus the minimum effective stress intensity  $K_{\text{min,eff}}$  in a cycle, under constant amplitude loading and under variable amplitude loading will produce the same crack extension (similarity concept).

### 2.1 Assumptions

Like any other crack closure model the McAir model is based on the assumption that crack growth behaviour is controlled by displacements within the plastic zone. These displacements are affected by crack surface contact behind the crack tip resulting from residual displacements left on the crack surface as the crack grows through prior plastic zones. The effect of crack surface contact during a load cycle is to restrict the change in crack opening displacements during the cycle, reducing the portion of the load cycle effective in propagating the crack [2]. With this concept crack growth retardation after overloads and acceleration after underloads can be explained.

It is assumed that for any load cycle, the load level at which closure occurs is a function of the highest peak load and lowest valley load which have occurred prior to that cycle. This assumption only holds if the applied load sequence is more or less random, however, with frequent occurrence of overloads. To provide for more-structured sequences, the 'highest' and 'lowest' load are regularly updated as the crack grows through the zone of plasticity caused by the overload. It is also assumed that the definition of a load cycle is unimportant, or, in other words, that it does not matter whether the minimum cyclic load precedes or succeeds the maximum load in the cycle. Again, this only holds for load sequences with frequent changes in load amplitude.

Unlike most other crack growth models, it is assumed that any stress variation, no matter how small, contributes to crack growth (provided that the maximum cyclic stress is greater than zero). In other words, it is assumed that some plastic deformation occurs at the crack tip even when the crack is only partially open. It is left to the user to eliminate insignificant cycles from the input load sequence.

The crack length that is used for the calculation of the stress intensity is assumed to be constant during a block of load cycles. This implies that the number of cycles in such a block should be limited to avoid inaccurate answers in case of highly loaded specimens.

No distinction is made between multiple and single overloads or underloads, so the effect of multiple overloads producing more retardation than a single overload is not accounted for.

### 2.2 Constant Amplitude Loading

The plastic deformations left in the wake of the crack tip cause the crack to close before complete

unloading. Under constant amplitude loading, the stress level at which this occurs is mainly a function of the applied stress ratio  $R$ , though stress state and material properties also play a role. From advanced analysis Dill and Saff [4,5] have derived the locus of these minimum effective stress intensity factors  $K_{\min,eff}$ . An example of such a stress ratio correction curve is given in figure 2.1. According to Dill and Saff this curve is lower for plane strain than for plane stress, higher for cyclic strain hardening materials, and lower for strain softening materials.

The equations that describe the stress ratio correction curve for a specific material have been derived from the listing of computer program CNTKM8 [6]. This program is the most recent version available to ARL of computer program CNTKSPC as described in reference [2]. According to [6] the minimum effective stress intensity factor  $K_{\min,eff}$  for a stress ratio  $R$  that is greater than or equal to zero is given by:

$$K_{\min,eff}/K_{\max} = x_r \cdot x_\alpha \cdot x_{fr} \quad (\text{for } R > 0) \quad (2.1a)$$

where

$$\begin{aligned} x_r &= 0.46733 + 0.29401R + 0.23866R^2 \\ x_\alpha &= 1 - (1 - \sqrt{\beta})(1 - R) \\ x_{fr} &= 1 - (0.756 - 0.912fr + 0.156fr^2)(1 - R) \\ \beta &= (\alpha + 1)/2 \end{aligned}$$

and  $K_{\max}$  is the stress intensity based on peak cyclic load. If the stress ratio is less than zero the minimum effective stress intensity can be found with:

$$K_{\min,eff}/K_{\max} = \text{effkr} \cdot e^{0.08R} + 0.225R \quad (\text{for } R < 0) \quad (2.1b)$$

where  $\text{effkr}$  is equal to the ratio  $K_{\min,eff}/K_{\max}$  as given by equation (2.1a) for a stress ratio  $R$  that equals zero. If equation (2.1) yield a minimum effective stress intensity  $K_{\min,eff}$  that is lower than zero or lower than the minimum stress intensity  $K_{\min}$  in the current cycle, then  $K_{\min,eff}$  is set equal to zero or  $K_{\min}$ , whichever is greater.

Parameter  $x_r$  relates the minimum effective stress intensity to the stress ratio  $R$ . It is similar to relations proposed by, or derived from, Elber [3], Schijve [7] and others.

Parameter  $x_\alpha$  accounts for the effect of material thickness. It depends on the retardation parameter  $\alpha$ , which is input by the user and ranges from -1 (no retardation) to +1 (maximum retardation). Theoretically, a value of zero pertains to the situation of plane strain while a value of +1 pertains to the state of plane stress around the crack tip. In practice, however, factor  $\alpha$  is used to tune the model.

Parameter  $x_{fr}$  brings into account the behaviour of the material under cyclic loading. It is a function

of ratio  $r$  between the cyclic and monotonic yield stress. Cyclic strain hardening behaviour will result in more retardation while cyclic softening will cause less retardation. This may be rather surprising since retardation usually is associated with the plastic zone size, which, in its turn, is inversely proportional to the yield stress. It should not be forgotten however, that the outer regions of the plastic zone cover areas that have hardly experienced reversed plasticity so the plastic zone size is principally related to the monotonic yield stress. Crack growth, on the other hand, is controlled by displacements within the plastic zone near the crack tip, where the material has experienced severe reversed plasticity. So crack growth will be determined by the cyclic behaviour of the material.

The minimum effective stress intensity  $K_{min,eff}$  as given by equation (2.1) is depicted in figure 2.2 as a function of  $R$  and  $\alpha$ . Figure 2.3 shows how  $K_{min,eff}$  varies with ratio  $r$ . Figure 2.4 shows how the McAir equations compare with equations proposed by Elber [3] and Schijve [7].

### 2.3 Variable Amplitude Loading

The stress ratio correction curve does not represent the behaviour at the crack tip under variable amplitude loading. The minimum effective stress intensity  $K_{min,eff}$  required to open the crack is not only determined by the stress ratio of the current cycle, but it also depends heavily on the highest and lowest load previously experienced.

Consider the simplified stress ratio correction curve of figure 2.1. The same curve is depicted in figure 2.5a again. In this figure, however, this curve represents the minimum effective stress intensity that would occur if the material were subject to a constant amplitude loading with maximum stress intensity  $K_{max,ol}$  and minimum stress intensity  $K_{min,ol}$ , where  $K_{max,ol}$  and  $K_{min,ol}$  are defined by a characteristic overload/underload combination prior to the current cycle of the actual sequence. The definition of these loads will be dealt with later on in this chapter. To find the minimum effective stress intensity  $K_{min,eff}$  of the current load cycle, point A on the stress ratio correction curve that is associated with the overload/underload combination is used as a starting point.  $K_{min,eff}$  is found by drawing a line with tangent 0.225 to point B that corresponds with the ratio  $K_{min}/K_{max,ol}$  on the abscissa, where  $K_{min}$  is the minimum applied stress intensity in the current cycle. It may well happen that the resulting minimum effective stress intensity  $K_{min,eff}$  is lower than zero or lower than the minimum applied stress intensity  $K_{min}$ , as is shown in figure 2.5c. In that case  $K_{min,eff}$  is assumed to be equal to zero or to  $K_{min}$ , whichever is greater. It should be noted that the ordinate represents the ratio of  $K_{min,eff}$  and  $K_{max,ol}$  and thus it is clear that the minimum effective stress intensity  $K_{min,eff}$  in the current cycle depends heavily on the overload  $K_{max,ol}$  that occurred before. A high overload will give a high value for  $K_{min,eff}$ . If the tangent of line AB were zero instead of 0.225 then  $K_{min,eff}$  would solely be determined by the overload/underload combination.

The effect of the underload is illustrated with figure 2.5b. If the underload goes down from  $K_{min,ol}$

to  $K_{\min,ol}$ , keeping  $K_{\min}$  and  $K_{\max,ol}$  at the same level, then the minimum effective stress intensity  $K_{\min,eff}$  goes down from B to B'. This reflects the effect of underloads to reduce crack closure. It is interesting to note that the tangent of the stress ratio curve for  $R < 0$  is approximately equal to 0.225, as can be seen in figure 2.2. This means that the actual magnitude of negative underloads does not really matter for crack growth acceleration.

A peculiar feature of the McAir model is the introduction of a maximum effective stress intensity  $K_{\max,eff}$ , analogous to the minimum effective stress intensity  $K_{\min,eff}$ . Usually  $K_{\max,eff}$  is equal to the maximum stress intensity that occurs in a cycle, as one would expect. If the overload is much higher than this maximum cyclic stress, however,  $K_{\max,eff}$  is calculated such that the effective stress intensity range  $\Delta K_{eff}$  in the cycle becomes equal to  $0.225 (K_{\max} - K_{\min})$ , where  $K_{\max}$  and  $K_{\min}$  are the actual cyclic stresses. In this way sustained crack arrest due to high overloads never occurs.

### 2.3.1 Definition of Overload and Underload

As already outlined the closure stress for a particular load cycle is mainly determined by a characteristic overload and underload which have occurred prior to that cycle. These loads are regularly updated as the crack grows through the plastic zone caused by the overload. The overload is adjusted to the maximum load in the current cycle if (1) the crack has grown through the plastic zone caused by the previous overload, or (2) the maximum stress intensity in a cycle exceeds the value of a variable named *check*. This variable is a function of the previous overload, the size of the associated plastic zone  $w_{ol}$  and crack length  $a_{ol}$ , and the current crack length  $a$ . This is shown in figure 2.6, which was derived from reference [6]. Also indicated in this figure, for comparison, is the stress intensity factor necessary to create a plastic zone that extends beyond the plastic zone as created by the previous overload. This curve was derived by assuming that the size of the plastic zone due to some arbitrary load is proportional to  $K^2$ , where  $K$  is the stress intensity associated with this load (see equation (2.2) in the next section).

In both above-mentioned cases the underload is updated as well. Apparently the physical reasoning behind this is that an overload erases the material's memory. The underload is also adjusted to the minimum load in the current cycle when the minimum stress intensity in a cycle is lower than the stress intensity  $K_{\min,ol}$  that is associated with the previous underload. In short:

$K_{\max,ol}$ is adjusted to $K_{\max}$ when	1. $a > a_{ol} + w_{ol}$
	2. $K_{\max} > \text{check}$
$K_{\min,ol}$ is adjusted to $K_{\min}$ when	1. $a > a_{ol} + w_{ol}$
	2. $K_{\max} > \text{check}$
	3. $K_{\min} < K_{\min,ol}$

The above set of criteria is summarized in figure 2.7, which shows a very simple flow diagram of the McAir model. The notation is the same as used throughout the computer program, and is explained in appendix A. Again, only the case of a through crack in a CCT-specimen is considered.

### 2.3.2 Thickness Effect

In theory the retardation parameter  $\alpha$  accounts for the stress state around the crack tip. A value of +1 would pertain to thin sheet material and a value of zero to thick specimens. Factor  $\alpha$  asserts its influence in two ways. First of all  $\alpha$  determines the locus of the stress ratio correction curve, as is clear from equation (2.1) and from figure 2.2. This means that  $\alpha$  affects crack growth under both constant and variable amplitude loading. Secondly factor  $\alpha$  determines the size of the plastic zone ahead of the crack tip. This directly affects crack growth after an overload, since the effect of an overload does not vanish until the crack has grown through the associated plastic zone.

To determine the importance of the stress ratio correction curve, we will first consider the case of no-load-interaction during spectrum crack growth. In that case the stress ratio correction curve is solely used to account for the stress ratio effect on the opening stress. The effect of  $\alpha$  on crack growth need not necessarily be very large then, although the range of curves in figure 2.2 suggests otherwise. This has to do with the way the McAir model treats the material crack growth curve. Starting point is the  $da/dN - \Delta K$  curve for a stress ratio  $R$  of zero, which must be input by the user of the model. The tabulated  $\Delta K$ -values are then transformed to  $\Delta K_{eff}$ -values with the help of equation (2.1), where the effective stress intensity range  $\Delta K_{eff}$  is equal to  $K_{max}$  minus  $K_{min,eff}$ . It is obvious from figure 2.2 that lower  $\Delta K_{eff}$ -values will be obtained for thin material ( $\alpha = 1$ ) than for thick material ( $\alpha = 0$ ). During the subsequent crack growth calculation  $\Delta K_{eff}$  is calculated for each block of cycles. Again it is obvious that lower values for  $\Delta K_{eff}$  will be obtained for thin material than for thick material. The associated  $da/dN$ -value then is found by interpolation in the previously obtained  $da/dN - \Delta K_{eff}$  table. Because factor  $\alpha$  affects both the input crack growth data and the stress intensity range due to an applied load cycle, the resulting effect on stress ratio correction is quite small. This is illustrated with the following example. Consider the fictitious though realistic  $da/dN - \Delta K$  data set as listed in the table below:

da/dN [m/cycle]	$(\Delta K)_{R=0}$ [MPa $\sqrt{m}$ ]	$\Delta K_{eff}$	
		$\alpha = 0$	$\alpha = 1$
$1 \cdot 10^{-9}$	3.0	2.0	1.6
$3 \cdot 10^{-6}$	30.0	20.0	16.0

The first two columns represent the input data for a stress ratio of zero while the last two columns represent the associated  $\Delta K_{eff}$  - values for two extremes of factor  $\alpha$  as calculated with equation (2.1a), with ratio  $f_r$  equal to one. Now consider an arbitrary load cycle with a stress ratio  $R$  of 0.5 and a stress intensity range  $\Delta K$  of 15.0 MPa $\sqrt{m}$ . Application of equation (2.1a) to this value yields an effective stress intensity range  $\Delta K_{eff}$  of 12.74 MPa $\sqrt{m}$  for  $\alpha$  equal to zero and 9.78 MPa $\sqrt{m}$  for  $\alpha$  equal to one respectively. Interpolation in the respective  $\Delta K_{eff}$  - columns of the above table, using the logarithm of the listed values as is usual, finally yields a growth rate  $da/dN$  of  $6.3 \cdot 10^{-7}$  m/cycle for  $\alpha$  equal to zero and  $5.5 \cdot 10^{-7}$  m/cycle for  $\alpha$  equal to one respectively. The difference between the calculated growth rates amounts to 13%, which is relatively small considering the fairly large spread between the stress ratio curves for the two extremes of factor  $\alpha$  (see figure 2.2). It can thus be concluded that it does not matter much what value for  $\alpha$  is used when correlating constant amplitude crack growth under arbitrary stress ratio to crack growth data for a stress ratio of zero, as long as factor  $\alpha$  is applied consistently. If this is not the case large errors should be expected.

An interesting consequence of the large spread between the various stress ratio correction curves is that the McAir model predicts different constant amplitude crack growth behaviour for thin specimens and thick specimens. Consider again the material crack growth curve for a stress ratio of zero that is given by the table above. Suppose this curve has been derived from tests on a thin specimen, so that the effective stress intensity range is given by the last column of this table. Now let us apply this crack growth curve to a thick specimen that is subjected to constant amplitude loading with a stress ratio equal to zero and a stress intensity range  $\Delta K$  of 3.0 MPa $\sqrt{m}$ . The effective stress intensity range  $\Delta K_{eff}$  then can be found with equation (2.1a), using a value for  $\alpha$  of zero, and is equal to 2.0 MPa $\sqrt{m}$ . Interpolation, using the logarithm of the listed values of the last and first column respectively, yields a crack growth rate  $da/dN$  of  $2.2 \cdot 10^{-9}$ , while a value of  $1.0 \cdot 10^{-9}$  would have been obtained for a thin specimen. It is not clear from publications whether such a large difference is realistic or not, but it is clear that care should be taken when choosing a crack growth curve for a specific problem.

Regarding variable amplitude loading, both the locus of the stress ratio correction curve and the size of the plastic zone are of importance. The equation that is used for the plastic zone size  $w_{ol}$  due to an overload  $K_{max,ol}$  is:

$$w_{ol} = \beta (\pi/8) (K_{max,ol} / \sigma_{y,eff})^2 \quad (2.2)$$

where

$$\beta = (\alpha + 1)/2$$

and  $\sigma_{y,eff}$  is some effective monotonic yield stress by which large scale net section yielding is accounted for. At lower stress levels  $\sigma_{y,eff}$  is approximately equal to the monotonic yield stress, while its value

drops drastically when the applied stress approaches the monotonic yield stress. This is shown in figure 2.8. Equation (2.2) yields a plastic zone size that is twice as large under plane strain as under plane stress. Usually this ratio is assumed to be equal to three [8]. It was already discussed in section 2.3.1 that in the case of a load sequence with infrequent changes in load amplitude the effect of an overload does not vanish until the crack has grown through the associated plastic zone. Thus the thickness of a specimen will play an important role in the process of crack growth retardation after an overload. This effect is promoted by the dependence of the minimum effective stress intensity  $K_{\min, \text{eff}}$  in an overload cycle (which is given by the stress ratio correction curve) on parameter  $\alpha$ . The higher the value of  $\alpha$ , or the smaller the specimen thickness, the higher the minimum effective stress intensity in the overload cycle, and thus the smaller the effective stress intensity range  $\Delta K_{\text{eff}}$  in subsequent cycles.

### 2.3.3 Examples

Two examples of the definition of overloads and underloads are given in figure 2.9. The consecutive overloads and underloads are indicated with arrows. The approximate location of the minimum effective stress intensity is indicated with a small cross. The initial overload/underload combination is determined by the first cycle, which is self-evident. According to the above criteria the second cycle in figure 2.9a yields a new overload, since the maximum stress intensity associated with this cycle will exceed the value of variable *check* (see figure 2.6). As a consequence a new underload is defined as well, since this is always coupled to the definition of a new overload. At the third cycle nothing happens. Even the minimum effective stress intensity remains the same, since  $K_{\min}$  equals  $K_{\min, \text{ol}}$ . The fourth cycle yields a new underload and the minimum effective stress intensity goes down as a consequence. The fifth cycle is dominated by the combination of the cycle 2 overload and the cycle 4 underload. The minimum effective stress intensity is higher than that of the fourth cycle, but it will not become as high as the minimum effective stress intensity of the third cycle.

The coupling of the definition of underloads to the definition of overloads can be rather loose in certain situations. This is illustrated in figure 2.9b. The effect of the severe underload at the second cycle is immediately cancelled out by the overload at the third cycle, which is not very realistic.

It should be noted that the McAir model does not explicitly bring into account the effect of multiple overloads producing more retardation than a single overload. This effect can only be arbitrarily accounted for by tuning the model with retardation parameter  $\alpha$ . It should also be noted that the effect of delayed retardation after a high overload is not included in the model.

### 3. ASSESSMENT OF THE MCAIR MODEL

#### 3.1 Experiments

To assess the McAir model use has been made of experimental data described in references [1] and [9]. These data were obtained from tests using several reconstitutions of a flight-by-flight fighter load sequence. This sequence was that used in fatigue testing a Mirage IIIO wing. It is typical of that for a fighter aircraft, covering 500 flights and consisting of 108,920 turning points. The maximum load corresponds to 7.5 g. Cycles in this sequence were counted using the range-pair method, giving a table of numbers corresponding to various peak-trough combinations. For the present work the original *flight-by-flight sequence* plus three artificial reconstitutions of this sequence were used: Two more-structured sequences were supposed to promote and retard crack growth. The *acceleration sequence* aimed at shortening of crack growth life, while the *retardation sequence* was developed to produce the longest possible crack growth life. These two sequences are shown in figure 3.1. The fourth reconstitution, the *random sequence*, was generated in a more or less random way. All sequences used returned the same range-pair table when counted. Information about the way these load sequences were generated can be found in reference [1].

Centre-cracked specimens of A7-U4SG-T651 aluminium alloy (equivalent to US alloy 2214) were tested under each of the four sequences described above. The specimens measured 12 mm x 80 mm x 300 mm, with a central spark-machined slit 0.015 mm wide by 12 mm in length. The specimens were pre-cycled to a crack length of 13.2 mm. The average test frequency was 5.5 Hz, and two gross-area stress levels of 11.09 and 17.00 MPa/g were employed to yield a range of test lives. More details about the specimens and the test procedures can be found in references [9] and [10].

The test results are presented in figure 3.2, which has been obtained from reference [1]. A remarkable result is that the acceleration sequence yielded the longest crack growth life under both stress levels. Furthermore, the differences in crack growth lives between those under the acceleration and the retardation sequences and also between those under the random and f-b-f sequences were quite small. Crack growth under the more-structured sequences (acceleration and retardation), however, is significantly slower than under the less-structured more-fluctuating sequences (random and f-b-f). The maximum difference in average crack growth lives was between those under the acceleration and random sequences and was an average of 1.59:1 at the stress level of 11.09 MPa/g, and 1.51:1 at 17.0 MPa/g.

#### 3.2 Constant Amplitude Data

The McAir model assumes that the constant amplitude  $da/dN - \Delta K$  curve that is input by the user is

for a stress ratio of zero. Only experimental data for stress ratio's -0.7, 0.2 and 0.7 were available for the A7-U4SG-T651 aluminium alloy however [11]. To overcome this problem an equation due to Schijve [7] was used to define an effective  $\Delta K$  in such a way that it correlates all the experimental data available. This equation had already been applied successfully in the past at ARL. It can be written as:

$$\Delta K_{\text{eff}} = (0.55 + 0.35R + 0.1R^2) \Delta K \quad (3.1)$$

This equation is represented in figure 2.4 by the 'Schijve (1)' - curve. Essentially this equation is similar to equation (2.1). Equation (3.1) showed better correlation between the constant amplitude data, however. With equation (3.1) the three sets of experimental data were transformed to one set of  $R = 0$  data. Using logarithmic scales a straight line was fitted through these data. This resulted in the following material curve, which is valid for crack growth rate in m/cycle and stress intensity in  $\text{Pa}\sqrt{\text{m}}$ :

$$\log(da/dN) = 3.7162 \log(\Delta K) - 33.158 \quad (\text{for } R = 0) \quad (3.2)$$

Two curves were added to this straight line to account for the growth rates outside the  $\Delta K$  data limits. These curves were fitted in a rather arbitrary way, taking care however that the tangent of these curves at the  $\Delta K$  data limits was equal to the tangent of the straight line through the data. The threshold value of the effective  $\Delta K$  was taken to be  $0.80 \text{ MPa}\sqrt{\text{m}}$  with  $da/dN$  equal to  $10^{-11}$  m/cycle, and the fracture toughness was taken as  $48.6 \text{ MPa}\sqrt{\text{m}}$  with  $da/dN$  equal to 1.0 m/cycle. These values were obtained from reference [10]. The resulting crack growth curve is shown in figure 3.3. The tabulated data are given in table 1. Table 2 gives the static properties of the material used. These data were obtained from references [10] and [12].

### 3.3 Predictions

Crack growth was predicted using the McAir model and the four sequences described in section 3.1, for the two stress scaling levels of 11.09 and 17.0 MPa/g. The  $da/dN - \Delta K$  data of table 1 and the static properties of table 2 were used. It was not clear what value for the input parameter  $\alpha$  should be used. Given the relatively large specimen thickness of 12 mm, a value of zero seemed appropriate since this value theoretically pertains to the situation of plane strain around the crack tip. Using various values for  $\alpha$  showed that much lower values yielded better predictions, especially for the stress scaling level of 11.09 MPa/g. It was felt that nothing is proved by getting excellent predictions due to an input parameter that was manipulated to suit experimental results. Therefore it was decided, rather arbitrarily, to use an  $\alpha$  value of -0.2 for both stress levels, as a compromise between experiment and theory. The computer program CNT8SHR, a modified version of the originally available computer program CNTKM8 [6], was

used for the calculations. This program is described in appendix A.

Predicted crack growths are shown in figure 3.4 for the four sequences and the two stress levels examined. In figure 3.5 the predictions from the McAir model are compared against the experimental crack growth data. This figure also shows the predictions for the unretarded or no-load-interaction-case. These latter predictions were made using a simple computer program that employed equation (3.1) to account for the stress ratio effect in each cycle. It would also have been possible to use computer program CNT8SHR, or CNTKM8, to make predictions for the unretarded case by inputting a value of -1 for  $\alpha$ . This would not have yielded the same results however, since no correction for the stress ratio is made if  $\alpha$  equals -1 and all cycles are treated as if the stress ratio were zero.

Table 3 summarizes the predicted crack growth lives for various values of retardation parameter  $\alpha$ . The predictions for the unretarded case are also listed. Note the difference between these latter predictions and the predictions with  $\alpha$  equal to -1. Table 4 essentially contains the same information as table 3, except that the predicted crack growth lives are presented as a percentage of the experimental crack growth life. In table 5 the predicted crack growth lives are compared against predictions made with three other crack growth models: the Wheeler model, the Willenborg model and the Modified Willenborg model. The numbers between brackets denote the predicted crack growth lives as a percentage of the experimental life. These data were obtained from reference [1]. The data are listed in the order of increasing predicted crack growth lives.

Several observations follow from the predicted data. Table 4 shows that predictions for the unretarded case were always less than experimental lives, the difference for the more-random sequences at the lower stress level being quite small, however. For these sequences at this stress level the predictions with the McAir model, with  $\alpha$  equal to -0.2, yielded poor results. The crack growth lives for these cases were grossly over-estimated by a factor of two. An interesting detail is that even with a value for  $\alpha$  as low as -1 the crack growth life is still over-estimated. The crack growth lives for the more-structured sequences at the lower stress level were predicted very well. The maximum deviation from the experimental results was 11%. The predictions over the whole range of sequences at the higher stress level were fairly good. The maximum difference between predicted and experimental lives, using a proportion greater than one, is 1.39:1 for the acceleration sequence. It should be realized that these results are highly affected by the value for input parameter  $\alpha$ . Apparently the value of -0.2 is very satisfactory for the stress scaling level of 17.0 MPa/g. For the stress level of 11.09 MPa/g a lower value for  $\alpha$  would be more appropriate to get a better average result over the whole range of load sequences. For reasons mentioned before no attempt has been made to optimize  $\alpha$  for this stress level however. In that respect the ranking of the predictions with the McAir model in table 5 should not be taken too absolutely.

Obtaining reasonable crack growth predictions may be important for normal engineering purposes, but whether or not the right trend is predicted is of much more importance when assessing a crack

growth model. In that respect it is interesting to compare the various predictions among themselves. Figure 3.4 shows that a longer crack growth life was predicted for the acceleration sequence than for the retardation sequence, though the difference is quite small. This is in agreement with the experimental data, as can be appreciated from figure 3.2. Comparison between the results for the more-random sequences also shows a good correlation between experimental and predicted trend. However, experimentally the acceleration sequence gave the longest crack growth life and the random sequences gave the shortest. Yet the McAir model predicted the reverse at both stress levels, as can be seen in figure 3.4. According to reference [1] the Wheeler model, the Willenborg model and the Modified Willenborg model showed the same behaviour.

### 3.4 Thickness Effect

It has been reported by various authors that the specimen thickness seriously affects the fatigue crack growth behaviour under variable amplitude loading, crack growth lives for thicker material being systematically shorter. Schijve [13] has given an overview of published results of flight simulation tests. He found differences of up to a factor 6.2 between the crack growth lives of thick and thin specimens, though the variation of this factor was large. Revill et al. [14] tested the effect of a single overload on subsequent crack growth behaviour in 2024-T3 aluminium. They found that the resulting delay in crack growth  $N_d$  was greater by a factor of 8.5 for 1.6 mm thick specimens than for 6.4 mm thick specimens. The magnitude of  $N_d$  depends on various factors like the magnitude of overload and subsequent cyclic loading, as can be appreciated from figure 3.6. This figure is due to De Koning and was obtained from reference [15]. It is clear that the delay of crack growth becomes significantly larger with increasing overload.

To check whether the McAir model correctly predicts the trend in experimental crack growth of thin specimens giving a longer delay after a single overload than thick specimens, a systematic analysis has been performed involving variation of retardation parameter  $\alpha$ , representing specimen thickness, and overload  $K_{\max,ol}$ . No attempt has been made to reproduce the experimental data as published in references [14] and [15]. Only the simple case of a through crack in an infinite sheet under  $R = 0$  loading has been considered. The material data as described in section 3.2 have been used. The crack dimension  $a_{ol}$  at the time of the overload was 12.73 mm, and the maximum stress  $\sigma_{\max}$  in the cycles following the overload was 50.0 MPa. Factor  $\alpha$  ranged from -0.4 to +1.0, with an increment of 0.2, and the overload ratio  $\sigma_{\max,ol}/\sigma_{\max}$  ranged from 1.05 to 2.95, where  $\sigma_{\max,ol}$  is the maximum stress in the overload cycle.

The results of the calculations are presented in figure 3.7. Eight curves are shown in this figure, each representing the crack growth delay period  $N_d$  as a function of the overload ratio for a specific value of  $\alpha$ . Several observations follow from these curves. The most striking feature of the curves is

their shape. The first part of each curve resembles a parabola, just like the curve of figure 3.6. Each curve, however, sharply bends down at a certain overload ratio to continue in a much straighter way. This even applies to the curve that is associated with  $\alpha = -0.4$ , though for this curve the kink falls outside the figure. The explanation is fairly simple and lies in the definition of the maximum effective stress intensity  $K_{\max, \text{eff}}$ . This stress intensity is normally equal to  $K_{\max}$ . With increasing overload the effective stress intensity range  $\Delta K_{\text{eff}} (= K_{\max, \text{eff}} - K_{\min, \text{eff}})$  in the subsequent cycles will decrease, and at some point it will happen that  $\Delta K_{\text{eff}}$  in the subsequent cycles becomes lower than  $0.225\Delta K$ . In that case  $K_{\max, \text{eff}}$  is calculated such that  $\Delta K_{\text{eff}}$  becomes equal to  $0.225\Delta K$ , irrespective of the magnitude of the overload. In this way sustained crack arrest is avoided and the crack will always grow through the plastic zone due to the overload. Since  $K_{\min, \text{eff}}$  for a certain overload ratio increases with increasing  $\alpha$ , as can be deduced from figure 2.2 and equation (2.1), the kink in the curve will occur at lower overload levels for higher values of factor  $\alpha$ .

It is not clear whether the second part of each curve represents the actual behaviour of a fatigue crack after a high overload. Evidence exists [16] that sustained crack arrest never occurs and that a fatigue crack always will grow further, however slow. This may explain why the authors of the McAir model introduced a minimum effective stress intensity range, though the value of  $0.225\Delta K$  seems somewhat artificial and may in practice depend on the specimen thickness as well.

If we disregard the effect of the minimum effective stress intensity range and only look at the first part of the curves, it is immediately clear that a thinner specimen (higher  $\alpha$ ) will show a much longer delay period after an overload than a thick specimen. Comparing the curves for  $\alpha = 0$  and  $\alpha = 1$  it is found that the difference between the predictions ranges from 3:1 for an overload ratio of 1.3 to 9:1 for an overload ratio of 1.7. This seems in agreement with the experimental results quoted before.

### 3.5 Discussion

The crack growth predictions for the structured sequences were quite satisfactory. A reasonable value for the retardation parameter  $\alpha$  (that is, a value close to zero) yielded reasonable predictions. This is not true for the random sequences however. For both stress levels the McAir model over-estimated the crack growth lives. Even a value of -1 for  $\alpha$  could not remedy this for the lower stress level. In fact, the experimental crack growth lives under the random load sequences at the stress level of 11.09 MPa/g were quite close to the no-load-interaction predictions, as can be appreciated from figure 3.5a. This effect was already observed by Schijve [17]. He found that load sequence effects only occur when changes in load amplitude are infrequent. In case of frequent load changes, the effect of overloads apparently is cancelled out immediately by frequently occurring underloads. This raises the question whether the effect of underloads is sufficiently being accounted for in the McAir model.

In the previous section the physical significance of the retardation parameter  $\alpha$  is emphasised. The

lower the value for  $\alpha$ , or the larger the specimen thickness, the shorter the crack growth delay after a single overload. This is entirely in accordance with experimental results. On the other hand, the results of the crack growth predictions suggest that the required value for  $\alpha$  also depends on the stress scaling level. Higher stress levels tend to require a higher value for this parameter. This illustrates the fact that it is necessary to use this factor as a tuning parameter in practice.

The assumption of the crack being stationary during a block of cycles has little effect on predicted crack growth life. As an example the crack growth life under the retardation sequence was calculated cycle-by-cycle for the no-load-interaction case. This sequence was the one with the fewest, and thus largest, blocks. The result is presented as a footnote in table 3. Compared with the 'normal' prediction the difference only amounted 3 %. Apparently the number of cycles in the blocks was still small enough to give sufficiently accurate results.

#### 4. ENHANCED CRACK CLOSURE MODEL

Although the McAir model predicted the crack growth lives under the structured sequences quite well, the results for the random sequences were fairly disappointing. Even more bothering was the fact that the experimental trend of the structured sequences giving the longest crack growth lives was not predicted correctly. It was felt that this was caused by the twofold combination of poor modelling of the underloads and inaccurate calculation of the effective stress intensity range during an overload cycle. This will be explained in the next paragraphs. To check this hypothesis a new model, the 'ARL model', was devised which finally resulted in computer program ARLECC (ARL Enhanced Crack Closure model). This present chapter describes the actual model, while the computer program is described and listed in appendix B.

##### 4.1 Actual Model

In conception the ARL model is very similar to the McAir model. The definition of overloads and underloads is nearly the same, and the handling of the stress ratio correction curve to obtain the minimum effective stress intensity in a cycle is practically equivalent. The retardation parameter  $\alpha$  has also been maintained, and is to be used in the same way. The main difference lies in the handling of the load sequence, the ARL model incorporating a cycle-by-cycle calculation, and the calculation of the minimum effective stress intensity in a cycle. Furthermore a number of details has changed, such as the calculation of the plastic zone size under plane strain.

#### 4.1.1 Constant Amplitude Loading

In principle, equation (2.1) can be used to correlate constant amplitude crack growth data for various values of stress ratio  $R$ . Applying these equations to the available  $da/dN$ - $\Delta K$  curves for the A7-U4SG-T651 aluminium alloy, however, yielded fairly poor results. This was already discussed in section 3.2. For this reason it was decided to employ another equation for the stress ratio correction curve. Two promising alternatives were available, both due to Schijve [7]. They are depicted in figure 2.4. These equations had already been shown to correlate experimental data very well. According to reference [18], the first one, denoted with 'Schijve (1)' and given by equation (3.1), gave the best results when applied to a particular set of constant amplitude data. The difference between the two equations was minimal, however. Since the second equation shows a more pronounced behaviour for negative  $R$ -values, as can be appreciated from figure 2.4, it was decided to employ this equation for the ARL model. It can be written as:

$$\Delta K_{\text{eff}} = (0.55 + 0.33R + 0.12R^2) \Delta K \quad (4.1)$$

Strictly speaking this equation is only valid for 2024-T3 aluminium alloy, since it was the result of regression analysis performed on a set of crack growth data for this material. According to reference [7], equation (4.1) may also be applied to 7075-T6 aluminium. In order to make this expression more generally applicable, and also to make use of the McAir experience on this subject, it was decided to incorporate correction factor  $x_{fr}$  of equation (2.1a) into the ARL model as well. This factor is to bring into account the behaviour of the material under cyclic loading. It is governed by the ratio  $fr$  between the cyclic and monotonic yield stress. According to reference [12], this ratio is approximately equal to 1.12 for both the 2024-T3 and the 7075-T6 aluminium alloy. To obtain a value of one for correction factor  $x_{fr}$  when applied to these two materials, this value of 1.12 was used to normalize the ratio  $fr$ . The expression for the stress ratio correction curve as used for the ARL model then became:

$$K_{\text{min,eff}}/K_{\text{max}} = x_r \cdot x_{fr} \quad (4.2)$$

where

$$\begin{aligned} x_r &= 0.45 + 0.22R + 0.21R^2 + 0.12R^3 \\ x_{fr} &= 1 - (0.756 - 0.912fr' + 0.156fr'^2)(1 - R) \\ fr' &= fr/1.12 \end{aligned}$$

The expression for  $x_r$  was simply derived from equation (4.1).

It may seem rather strange that parameter  $x_r$  has been included in equation (4.2), while parameter

$x_{\alpha}$  of equation (2.1) is not employed. In section 2.3.2 it was shown that the latter parameter may give rise to large differences in crack growth rate when used to transform thin specimen constant amplitude data to thick specimen data, and vice versa. It is not clear whether this is realistic or not. Publications on the effect of thickness on crack growth rate are sometimes contradictory, even when due to the same author [13,19]. This is why parameter  $x_{\alpha}$  was not included in the ARL model, though a deeper investigation may be worthwhile.

It must be noted here that the growth rate curve for the A7-U4SG-T651 aluminium alloy, described in section 3.2, was not corrected for the cyclic yield stress. The only reason for this is, that the growth rate curve was derived before much was known about the McAir model.

#### 4.1.2 Variable Amplitude Loading

As for variable amplitude loading, the ARL model differs from the McAir model on two important points. The first point concerns a peculiarity that is inherent to the way in which load blocks are handled by the McAir model. The second point concerns the minimum effective stress intensity in a load cycle in relation to the overload/underload combination that occurred prior to that particular load cycle.

The first point is best explained from figure 4.1. This figure shows a lo-hi stress sequence that consists of two load blocks. The dashed line indicates the minimum effective stress intensity in a cycle. Since the McAir model operates on blocks rather than on individual cycles, the minimum effective stress intensity will be constant within a block and the effective stress intensity range  $\Delta K_{eff}$  of the first cycle of the block will be as indicated in the upper part of figure 4.1. This behaviour is not very realistic, however, for the material will not 'feel' that a new block of cycles has started until point A is reached. The situation that is depicted in the lower part of figure 4.1 seems more realistic, and was therefore adopted for the ARL model. For this purpose the minimum effective stress intensity  $K_{min,eff}$ , and also the crack increment  $\Delta a$  for that matter, is calculated cycle-by-cycle in the ARL model. The effective stress intensity range  $\Delta K_{eff}$  then is calculated as the maximum stress intensity  $K_{max}$  in the current cycle minus the minimum effective stress intensity in the *previous* cycle.

This procedure may seem rather trivial if very structured sequences are considered with many load cycles per block. It does not really matter then how accurately the effective stress intensity range in the first cycle of each block is calculated. This is not true if crack growth is mainly caused by overloads, however, since they are most likely grouped in small blocks. In that case inaccurate calculation of the effective stress intensity in the first cycle may well affect the overall result. In that respect table 6 is of much interest. This table shows the contribution of overloads to crack growth for the load sequences that were used in testing the McAir model. The number of overloads as a percentage of the total number of cycles is also listed. For reasons of convenience this table was produced using the ARL model. This does not matter much, however, since the definition of overloads in both models is practically identical. Each

time two figures are listed, indicating a range of values that is covered while the crack grows. The first figure describes the situation just after crack growth started, and the second figure is associated with the critical crack length. The first figure is more important, since it describes about 80% of the crack growth life. For instance, the contribution of overloads to crack growth for the f-b-f sequence with a stress level of 11.09 MPa/g started at 9% and went up slowly to 12% at 80% of the crack growth life, and only after that it quickly went up to 25% at failure. It may seem rather strange that the relative number of overloads should vary with the crack length. It must be realized, however, that a new overload is defined when the crack has grown through the plastic zone due to the previous overload. Since the plastic zone size is proportional to  $K_{max}^2$ , and crack growth approximately to  $\Delta K^4$ , it is not surprising that the relative number of overloads increases with increasing crack length. From table 6 it can be concluded that crack growth under the retardation sequence is dominated by overloads, while overloads play a moderately important role under the remaining sequences. Thus, the new approach of using the minimum effective stress intensity of the previous cycle when calculating  $\Delta K_{eff}$  seems justified.

The second point on which the ARL model differs from the McAir model regarding variable amplitude loading, is best explained from figure 4.2. This figure is equivalent to figure 2.5, which applies to the McAir model. For a specific material, the minimum effective stress intensity in the current cycle is only a function of the previous overload/underload combination, as opposed to the McAir model, where the minimum effective stress intensity is also a function of the current stress ratio. The difference in result when applying both models to a certain load sequence is also indicated in figure 4.2. According to the McAir model, the minimum effective stress intensity in the cycles following an overload will go up with increasing stress ratio, while the ARL model will predict the minimum effective stress intensity to remain constant. It is not obvious why the designers of the McAir model have decided to make the minimum effective stress intensity a function of the stress ratio of the current cycle. There is no apparent physical argument for this, though the reason may have been to avoid the maximum effective stress intensity range  $\Delta K_{eff}$  to become greater than the nominal stress intensity range  $\Delta K$  in a cycle. In the ARL model this is avoided by including an 'if-statement' in the computer code that sets  $\Delta K_{eff}$  equal to  $\Delta K$  whenever the latter is exceeded. An exception to this rule is the first cycle of a block, as is explained in figure 4.3. It may be clear from comparison of figures 2.5 and 4.2 that the effect of underloads is more emphasised by the ARL model than by the McAir model.

Overloads and underloads in the ARL model are updated in the same way as described in section 2.3.1 for the McAir model. Two minor differences are that (1) the update criterion *check* is given by the dashed line in figure 2.6, and (2) the size of the plastic zone due to an overload is given by:

$$w_{ol} = (\beta/\pi)(K_{max,ol}/\sigma_{y,eff})^2 \quad (4.3)$$

where

$$\beta = 0.333 + 0.5\alpha + 0.167\alpha^2$$

In this way the plastic zone under plane strain is three times larger than under plane stress. According to reference [8], from which equation (4.3) was derived (except for  $\sigma_{y,eff}$ , which was obtained from [6]), this is more common than the factor of two that is used in the McAir model. The equation for  $\beta$  simply evolved from the desire that a value for  $\alpha$  of zero corresponds to plane stress, a value of one to plane strain, and a value of minus one to minimum retardation ( $\beta=0$ ), as is also the case for the McAir model. It should be realized that factor  $\alpha$  (and  $\beta$  for that matter) is only used for the calculation of the plastic zone size, while the McAir model also applies this factor in the determination of  $K_{min,eff}$ , as can be appreciated from equation (2.1).

Unlike the McAir model, the ARL model does not incorporate a maximum effective stress intensity factor. This implies that sustained crack arrest after a high overload can occur, as far as the ARL model is concerned. Like the McAir model, the ARL model does not distinguish between single and multiple overloads.

#### 4.2 Predictions

Crack growth was predicted using program ARLECC and the four sequences described in section 3.1, for the two stress scaling levels of 11.09 and 17.00 MPa/g. Again the material properties of tables 1 and 2 were used. Given the rather large specimen thickness a value of zero was used for input parameter  $\alpha$ .

Predicted crack growths are shown in figure 4.4 for the four sequences and the two stress levels examined. In figure 4.5 the predictions from the ARL model are compared against the experimental crack growth data. This figure also shows the predictions for the unretarded or no-load-interaction case. These latter predictions were made using the associated option of program ARLECC. This option involved the use of equation (4.2) to account for the stress ratio effect in each cycle. The predicted crack growth lives are summarized in tables 7 and 8, which are equivalent to tables 3 and 4 for the McAir model. In principle, the corresponding values of the no-load-interaction predictions in tables 3 and 7 should be equal. Since the ARL model calculates crack growth cycle-by-cycle, and because this model incorporates a different stress ratio correction curve, the results differ slightly however.

The crack growth lives were predicted quite well for both stress levels. The maximum difference between predicted and experimental lives is 1.28:1 for the random sequence at a stress level of 11.09 MPa/g, and 1.39:1 for the acceleration sequence at 17.00 MPa/g. Apparently the theoretical value of zero for input parameter  $\alpha$  was very appropriate, hence no sensitivity analysis of predicted crack growth to  $\alpha$  was undertaken. The most important observation, however, is that the experimental trend of the structured sequences giving the longest crack growth lives was predicted correctly. As such, the ARL

model is superior to other models examined so far.

To check whether the ARL model predicts the experimental trend of thin specimens showing a longer delay in crack growth after a single overload than thick specimens, computer program ARLECC was used to analyze the configuration that is described in section 3.4. Again a single overload was considered, followed by constant amplitude  $R = 0$  loading with a maximum cyclic stress  $\sigma_{\max}$  of 50 MPa. Only two values for  $\alpha$  were considered, namely zero and one.

The results of the calculations are presented in figure 4.6. The corresponding results from the McAir model are also included in this figure. Again the experimental trend is predicted correctly. The delay period  $N_d$  after an overload is approximately three times longer for thin specimens ( $\alpha = 1$ ) than for thick specimens ( $\alpha = 0$ ). This value is directly related to the difference in plastic zone sizes, since the stress ratio correction curve does not change with factor  $\alpha$ . Unlike the McAir model, the ARL model predicts sustained crack arrest after very high overloads. The shut-off ratio  $\sigma_{\max,ol}/\sigma_{\max}$  at which this occurs can be derived from equation (4.2) and is given by:

$$(\sigma_{\max,ol}/\sigma_{\max})_{\text{shut-off}} = \frac{1}{x_r \cdot x_{fr}} \quad (4.4)$$

Equation (4.4) is independent of factor  $\alpha$ . For the current example this equation yields a shut-off ratio of 2.54. According to figure 4.6, however, overload ratios greater than two already give very long delay periods. It is interesting to note that the shut-off ratio in figure 3.6 is equal to approximately 2.7. This supports the ARL model, although a different material under slightly different conditions was considered in this figure.

In the McAir model the stress ratio correction varies with the specimen thickness, whereas this curve is independent of  $\alpha$  in the ARL model. Together with the difference in calculation of the plastic zone size, compare equations (2.2) and (4.3), this explains the difference between the McAir curves and the ARL curves in figure 4.6. The 'straight' part of the McAir curves was already explained in section 3.4.

### 4.3 Discussion

For both stress levels examined, the predictions from the ARL model were quite good. Apparently the theoretical value of zero for input parameter  $\alpha$  was quite appropriate. The experimental trend of the structured sequences giving longer crack growth lives was predicted correctly. The effect of specimen thickness on spectrum crack growth, as described in the literature, was also predicted correctly.

Comparison of tables 3 and 7 shows that the results from the McAir model and the ARL model differ mainly for the more-random sequences, the ARL results being only about 58% of the corresponding McAir results. This is mainly caused by the more pronounced effect of underloads on

crack growth in the ARL model. It is true that the ARL model differs on more points from the McAir model, but it can be made plausible that these points are not very important in explaining the difference in results from the two models. Firstly, the ARL model uses the minimum effective stress intensity of the *previous* cycle to calculate the effective stress intensity range in the current cycle, as shown in figure 4.1. It was argued in section 4.1.2 that this is only important if crack growth is mainly determined by overloads that occur in small blocks of only a few cycles. It was shown that this was not the case for the random and the f-b-f sequence. For these sequences, overloads only determined about 10 to 20% of crack growth, depending on the stress level. This is not enough to explain the large differences between the results from the two models. In fact, only crack growth under the retardation sequence was mainly determined by overloads, see table 6, but these overloads were mainly grouped in large blocks, as can be appreciated from figure 3.1b.

Secondly, the ARL model employs a different stress ratio correction curve, together with a different equation for the plastic zone size. From figure 4.6 it follows that for a thick specimen the ARL model predicts more crack growth delay after a single overload than the McAir model. This indicates that the use of the new stress ratio correction curve, together with the different equation for plastic zone size, gives rise to *more* crack growth retardation in thick specimens under variable amplitude loading instead of *less*, as suggested by the difference between tables 3 and 7. This leaves the difference in modelling of the underloads as the only explanation why the ARL model gave better results than the McAir model. It was already shown in table 3 that the assumption of the crack being stationary during a load block had little effect on the accuracy of the results.

## 5. CONCLUSIONS

The following conclusions may be drawn from the previous sections, which tested the McAir model against experimental crack growth that covered several sequences and two stress scaling levels. It must be realized that these conclusions pertain to a particular version of the McAir model, dating back to 1984. Later versions, which unfortunately were not available to ARL at the time this report was written, may have been drastically revised.

1. The McAir model predicted crack growth under the more-structured sequences quite well.
2. The more-random sequences were handled less well by the McAir model. Very unconservative results were obtained. Even a value as low as -1 for input parameter  $\alpha$  could not remedy this for the lower stress level. This is caused by poor modelling of the effect of underloads in the McAir model.
3. The trend in experimental crack growth of the more-structured sequences giving longer lives than

---

the more-random sequences was not predicted correctly. In this respect, the McAir model is not better than simpler models like the Wheeler model and the Modified Willenborg model.

4. Input parameter  $\alpha$  is the only parameter that can be used to tune the McAir model. This parameter was shown to represent the specimen thickness and, as such, has some physical significance. Higher stress levels tend to require a higher value for this parameter, however.

5. A proposed ARL model, based somewhat on the McAir model, predicted crack growth under the four load sequences and the two stress levels quite well. It is the only model examined so far on these data that correctly predicted the experimental trend of the more-structured sequences giving the longest crack growth lives. For the basic option of a through crack in a CCT-specimen, the proposed ARL model is superior to the McAir model.

6. The experimental trend of thin specimens showing longer crack growth delay after a high overload than thick specimens was predicted correctly by both models. Unlike the ARL model, the McAir model predicts that no sustained crack arrest will occur after a very high overload.

7. Neither model accounts for the effect of multiple overloads. The same applies to the phenomenon of delayed retardation after an overload.

## REFERENCES

1. Finney, J.M. and Machin, A.S. 'A test of some fatigue crack growth prediction models', Paper presented on the Symposium of the Australian Fracture Group, 1986.
2. Leist, R.T. and Saff, C.R. 'CNTKSPC user's manual - Contact stress model fatigue crack growth computer program', McDonnell Douglas Report MDC IR0245, March 1981.
3. Elber, W. 'The significance of fatigue crack closure', in Damage Tolerance in Aircraft Structures, ASTM STP 486, American Society for Testing and Materials, 1971.
4. Dill, H.D. and Saff, C.R. 'Spectrum crack growth prediction method based on crack surface displacement and contact analysis', in Fatigue crack growth under spectrum loads, ASTM 595, American Society for Testing and Materials, 1976.
5. Dill, H.D. and Saff, C.R. 'Analysis of crack growth following compressive high loads based on crack surface displacements and contact analyses', in Cyclic stress-strain and plastic deformation aspects of fatigue crack growth, ASTM 637, American Society for Testing and Materials, 1977.
6. Anonymous Listing of computer program 'CNTKM8'. Written in FORTRAN, 1984.
7. Schijve, J. 'Some formulas for the crack opening stress level', in Engineering Fracture Mechanics, volume 14, pp. 461 - 465, 1981.
8. Brock, D. 'Elementary Engineering Fracture Mechanics', third revised edition, Martinus Nijhoff Publishers, The Netherlands, 1984.

- 
9. Finney, J.M. and Denton, A.D. 'Cycle counting and reconstitution, with application to the aircraft fatigue data analysis system', C282/86, IMechE 1986.
  10. Finney, J.M., Harris, F.G., et al. 'Modelling for fatigue crack growth prediction in Mirage IIIO frame 26', ARL-STRUC-REPORT-401, Melbourne, Australia, April 1984.
  11. Dentry, C.S. 'Description and illustration of the use of CRACKS IV', ARL-STRUC-TM-389, Melbourne, Australia, August 1984.
  12. Anonymous R629.11 / SOC VOL. 1 86/8908, Society of Automotive Engineers SAE, Handbook 1986 Vol. 1 - Materials.
  13. Schijve, J. 'The significance of flight simulation fatigue tests', in Durability and damage tolerance in aircraft design, 13th ICAF symposium in Pisa, Italy, 1985.
  14. Reville, G.W., Ningaiah, and Finney, J.M. 'Load interaction effects in fatigue crack propagation', Aircraft Structural Fatigue, proceedings of a symposium held in Melbourne, ARL-STRUC-REPORT-363, Melbourne, Australia, October 1976.
  15. Padmadinata, U.H. 'Investigation of crack-closure prediction models for fatigue in aluminum alloy sheet under flight-simulation loading', Report LR-619, Delft University of Technology, Faculty of Aerospace Engineering, The Netherlands, March 1990.
  16. Finney, J.M. Aeronautical Research Laboratory, Melbourne, Australia, 1991 (private conversation).
  17. Schijve, J. 'Effect of load sequences on crack propagation under random and program loading', in Engineering Fracture Mechanics, volume 5, pp. 269 - 280, 1973.

18. Finney, J.M. and Deirmendjian, G. 'ΔK-effective: Which Formula ?', accepted for publication in *Fatigue & Fracture of Engineering Materials & Structures*.
19. Broek, D. and Schijve, J. 'The influence of sheet thickness on crack propagation', in *Aircraft Engineering*, volume 38, pp. 31 - 33, 1966.

$\Delta K$ (MPa $\sqrt{m}$ )	da/dN (m/cycle)
1.45455	1.000000 $\cdot 10^{-11}$
1.71190	4.000000 $\cdot 10^{-11}$
2.20198	1.993473 $\cdot 10^{-10}$
3.09742	9.201416 $\cdot 10^{-10}$
26.9774	2.864725 $\cdot 10^{-6}$
33.0770	8.310194 $\cdot 10^{-6}$
37.0996	2.461269 $\cdot 10^{-5}$
39.9125	7.389003 $\cdot 10^{-5}$
41.9771	2.238263 $\cdot 10^{-4}$
44.2058	1.193590 $\cdot 10^{-3}$
45.7876	6.425438 $\cdot 10^{-3}$
46.9660	3.481965 $\cdot 10^{-2}$
47.8767	1.896133 $\cdot 10^{-1}$
48.6000	1.0

Table 1. Crack growth curve for A7-U4SG-T651 aluminium alloy, stress ratio R = 0.

Young's modulus	69000 MPa
Monotonic yield stress	457 MPa
Cyclic yield stress	411 MPa
Fracture toughness <sup>o)</sup>	48.6 MPa $\sqrt{m}$

<sup>o)</sup> Induced from fatigue tests. A static test yielded 32.4 MPa $\sqrt{m}$ .

Table 2. Static properties of A7-U4SG-T651 aluminium alloy.

stress scale [MPa/g]	$\alpha$	calculated life [programs]			
		acceleration	retardation	f-b-f	random
11.09	0.0	48.0	47.0	58.3	57.7
	-0.2	43.2	43.0	52.7	52.3
	-1.0	26.5	26.9	30.8	31.2
	unretarded	21.0	21.7 <sup>*)</sup>	23.4	23.4
17.00	0.0	9.0	8.0	11.2	11.1
	-0.2	8.0	8.0	10.2	10.0
	-1.0	5.0	5.9	6.1	6.2
	unretarded	4.0	4.8	4.6	4.6

<sup>\*)</sup> 21.0 if calculated cycle-by-cycle

Table 3. Crack growth lives as predicted with the McAir model for various values of  $\alpha$ .

stress scale [MPa/g]	$\alpha$	relative life (% of experimental life)			
		acceleration	retardation	f-b-f	random
11.09	0.0	119	121	214	226
	-0.2	107	111	194	205
	-1.0	65	70	113	122
	unretarded	52	56	86	92
17.00	0.0	81	84	144	151
	-0.2	72	84	130	136
	-1.0	45	62	78	84
	unretarded	36	51	59	62

Table 4. Predicted crack growth lives as a percentage of the experimental crack growth life (McAir model).

stress scale [MPa/g]	load sequence			
	acceleration	retardation	f-b-f	random
11.09	Un (52) Wh (62) MW (71) <i>Mc</i> (107) Wi (108)	Un (56) Wh (59) MW (69) Wi (98) <i>Mc</i> (111)	Un (86) Wh (111) MW (144) <i>Mc</i> (194) Wi (235)	Un (92) Wh (122) MW (154) <i>Mc</i> (205) Wi (268)
17.00	Un (36) MW (63) Wh (64) <i>Mc</i> (72) Wi (76)	Un (51) Wh (62) MW (70) <i>Mc</i> (84) Wi (88)	Un (59) Wh (125) <i>Mc</i> (130) MW (138) Wi (169)	Un (62) Wh (132) <i>Mc</i> (136) MW (149) Wi (180)

Un no-load-interaction  
 Wh Wheeler model  
 Wi Willenborg model  
 MW Modified Willenborg model  
 Mc McAir model ( $\alpha = -0.2$ )

Table 5. Comparison of predicted crack growth lives. Figures indicate percent of experimental crack growth life. Data obtained from reference [1].

stress scale [MPa/g]	[%]	load sequence			
		acceleration	retardation	f-b-f	random
11.09	$N_{ol}/N_{total}$	0.3 - 0.6	1.6 - 3.1	0.3 - 0.5	0.3 - 0.5
	$\Delta a_{ol}/\Delta a_{total}$	10 - 35	49 - 79	9 - 25	9 - 23
17.00	$N_{ol}/N_{total}$	0.7 - 1.1	3.5 - 4.8	0.6 - 0.8	0.5 - 0.9
	$\Delta a_{ol}/\Delta a_{total}$	19 - 39	74 - 87	14 - 31	16 - 39

$N_{ol}$  total number of overloads already experienced  
 $N_{total}$  total number of cycles already experienced  
 $\Delta a_{ol}$  total crack growth due to overloads  
 $\Delta a_{total}$  total crack growth

Table 6. Contribution of overloads to crack growth (calculated using ARL model).

stress scale [MPa/g]	$\alpha$	calculated life [programs]			
		acceleration	retardation	f-b-f	random
11.09	0.0 unretarded	41.0	39.0	34.2	32.7
		21.0	21.0	23.6	23.5
17.00	0.0 unretarded	8.0	8.0	6.8	6.5
		4.0	4.0	4.7	4.7

Table 7. Crack growth lives as predicted with the ARL model.

stress scale [MPa/g]	$\alpha$	relative life (% of experimental life)			
		acceleration	retardation	f-b-f	random
11.09	0.0 unretarded	101	101	126	128
		52	54	87	92
17.00	0.0 unretarded	72	84	87	87
		36	42	60	63

Table 8. Predicted crack growth lives as a percentage of the experimental crack growth life. The final life was used for comparison (ARL model).

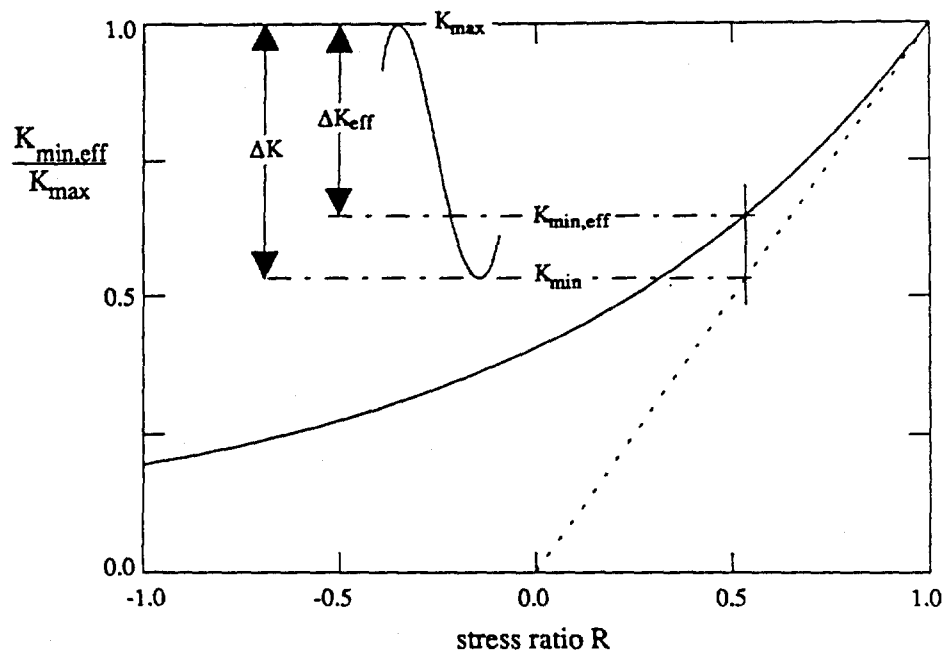


Figure 2.1 Generic stress ratio correction curve.

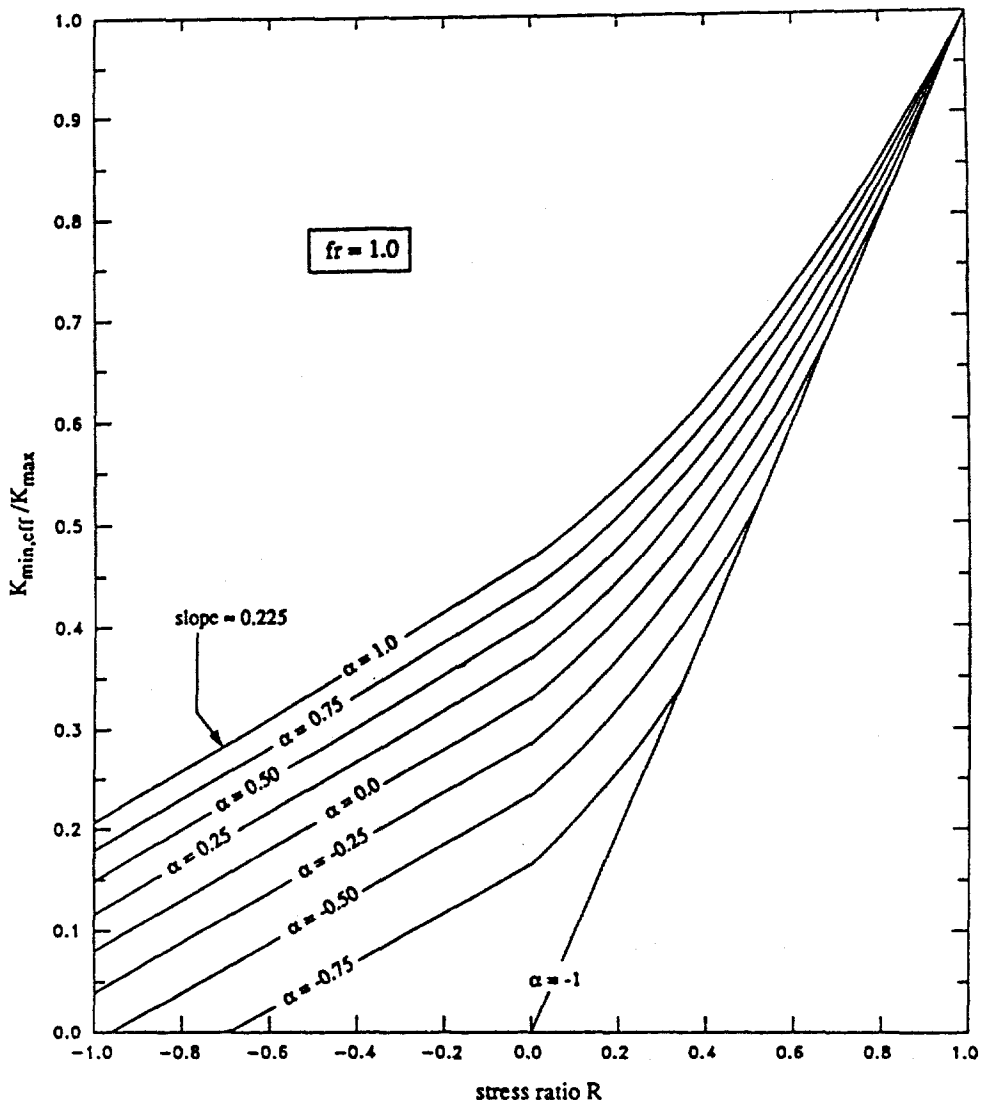


Figure 2.2 McAir stress ratio correction curves as a function of retardation parameter  $\alpha$ , for a ratio  $fr$  between cyclic and monotonic yield stress of 1.0.

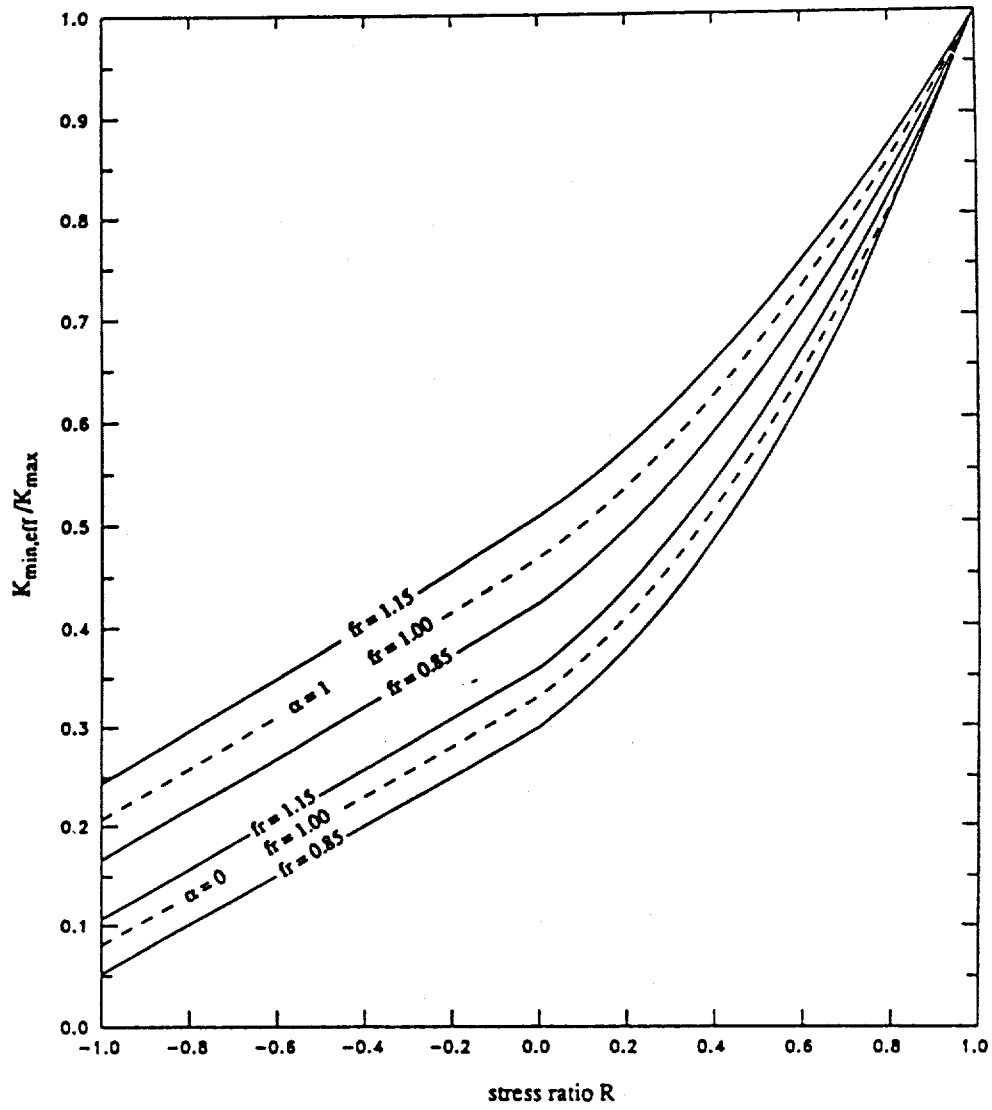


Figure 2.3 Variation of the McAir stress ratio correction curves with ratio  $f_r$  between cyclic and monotonic yield stress.

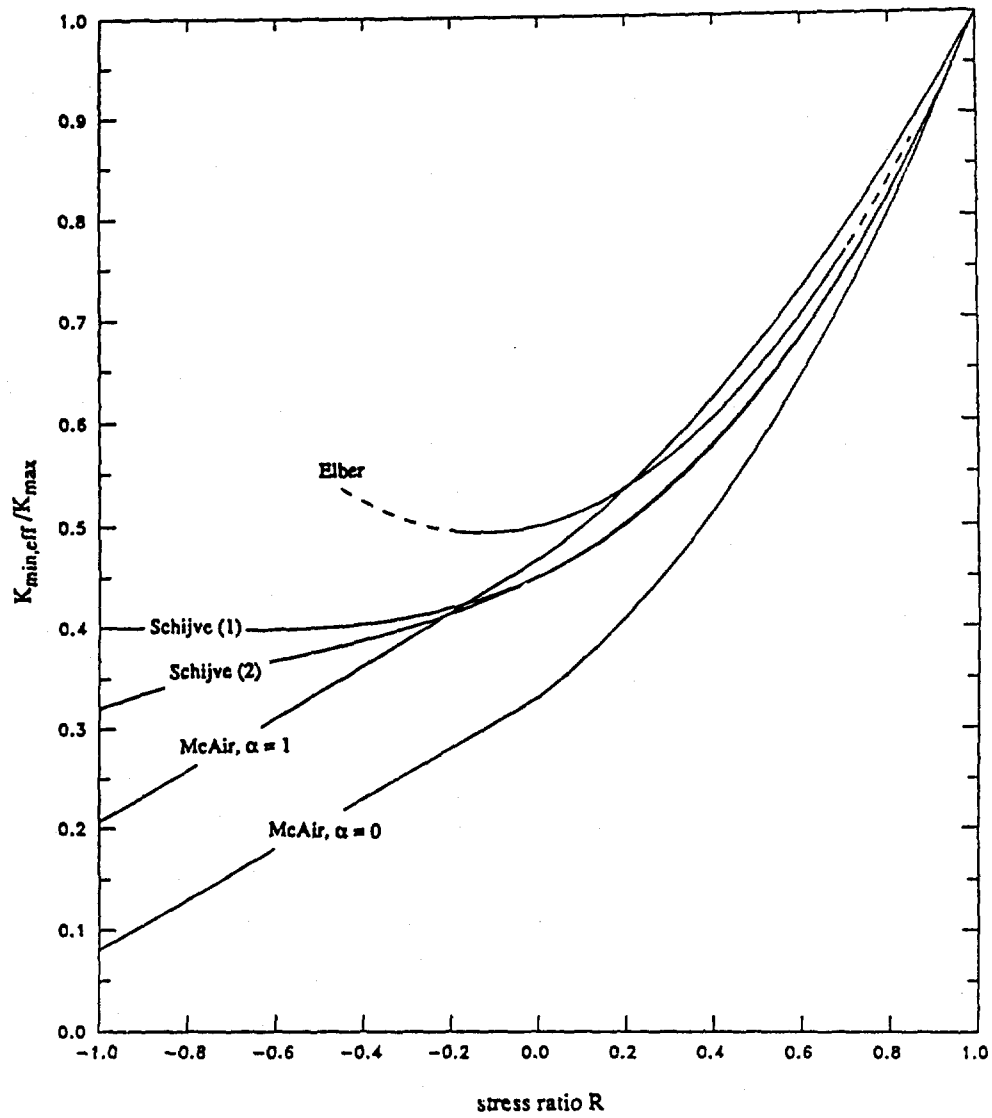


Figure 2.4

Comparison between the McAir stress ratio correction curves and similar curves due to Elber [3] and Schijve [7].

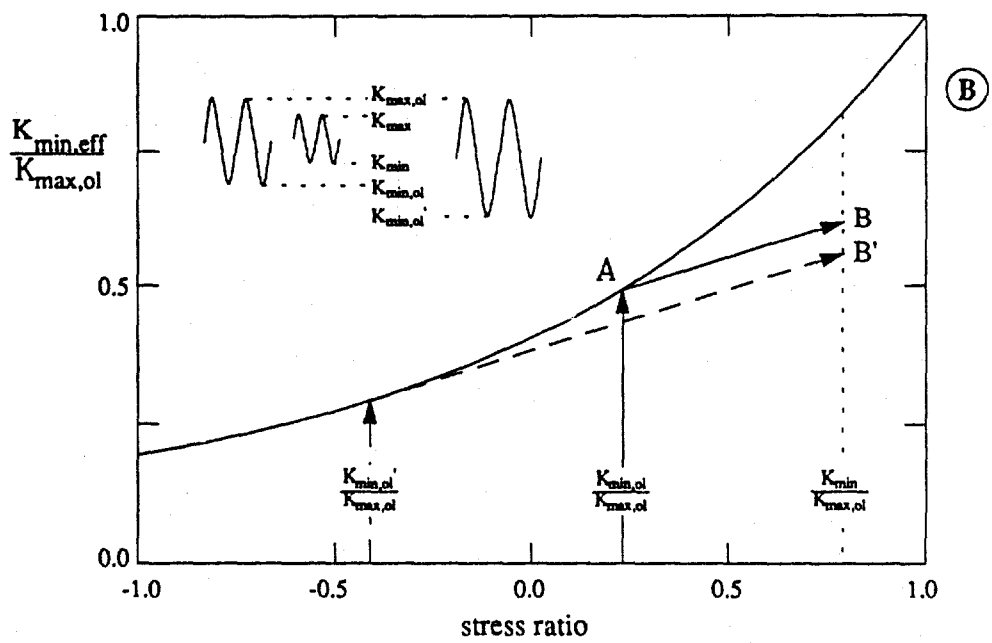
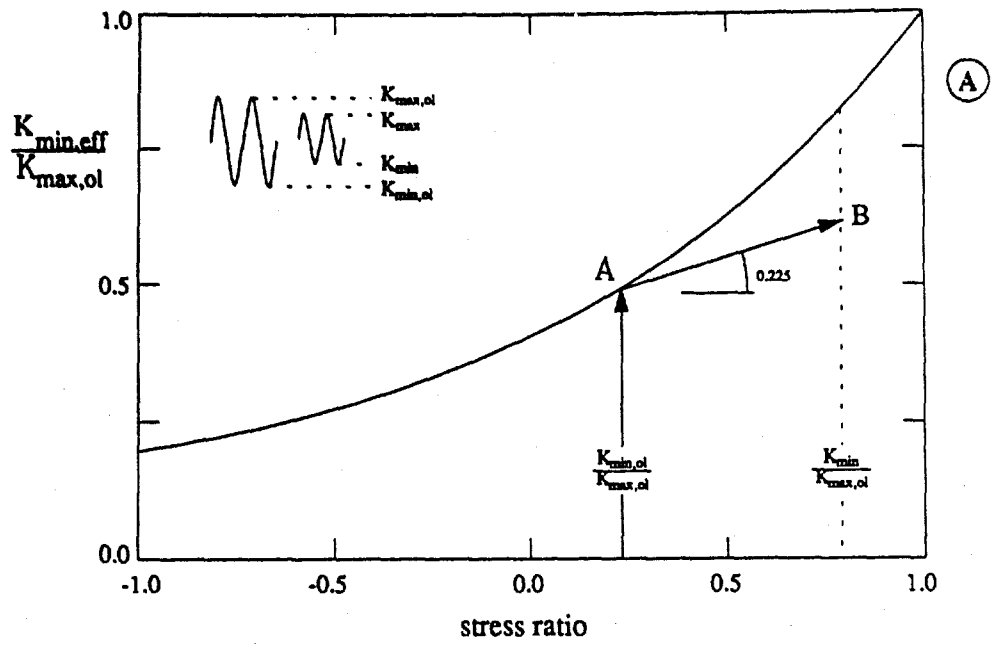


Figure 2.5 Calculation of the minimum effective stress intensity  $K_{min,eff}$  under variable amplitude loading (McAir model).

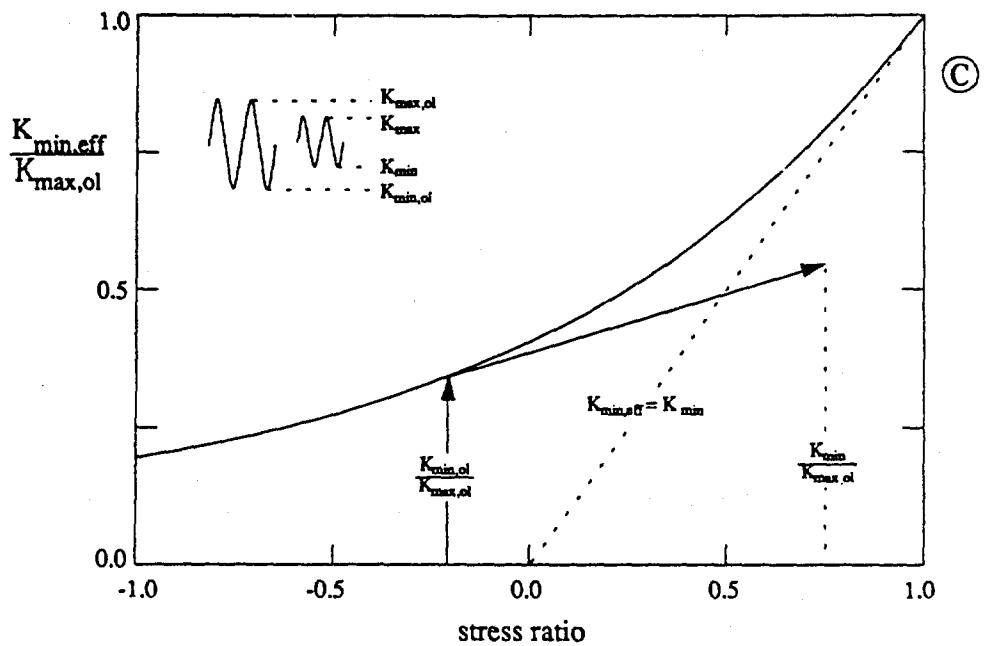


Figure 2.5 (continued).

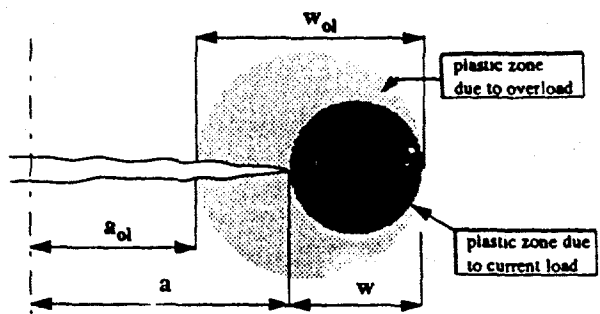
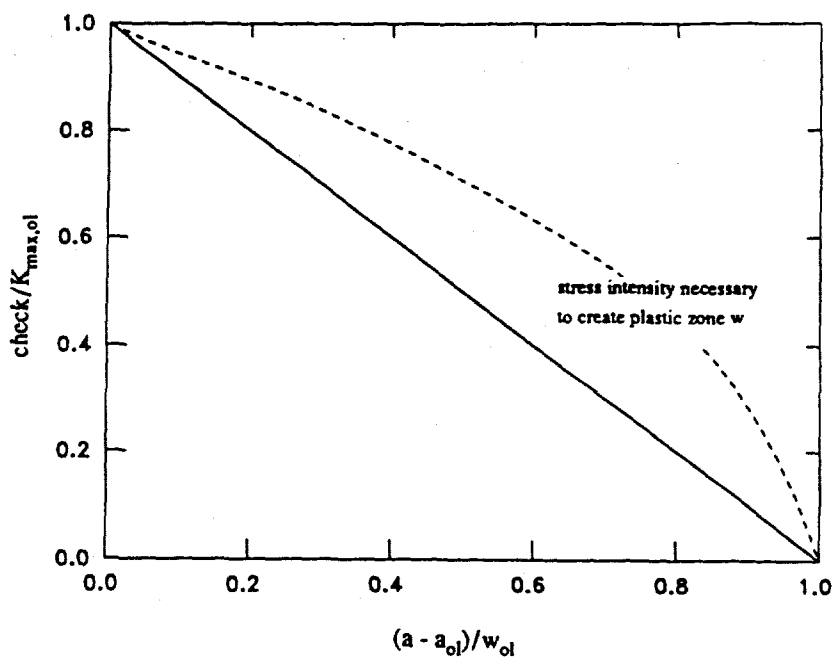


Figure 2.6 Parameter *check* as a function of the crack length. The effect of large scale yielding has been disregarded in this figure.

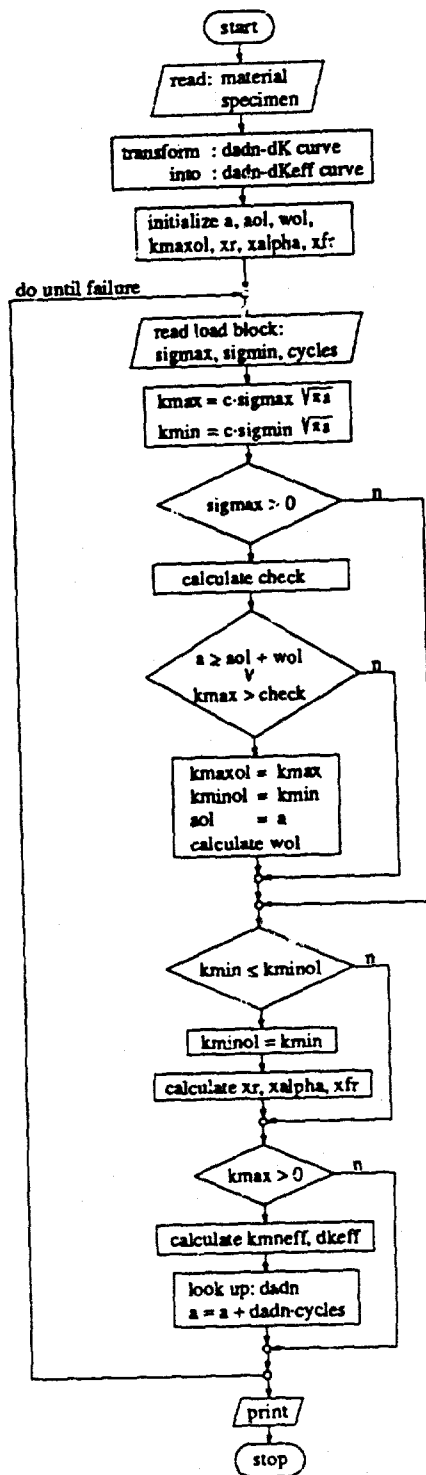


Figure 2.7 Simple flow diagram of the McAir model, covering the case of a through crack in a CCT-specimen.

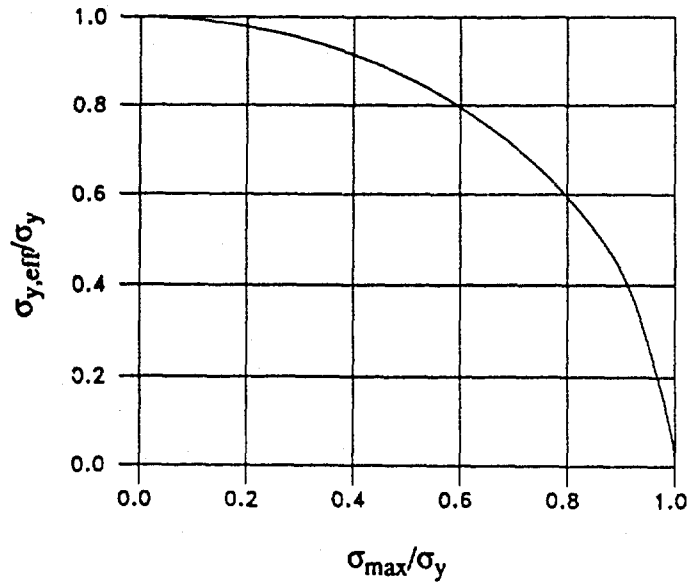


Figure 2.8 Effective monotonic yield stress  $\sigma_{y,\text{eff}}$  as a function of applied gross stress  $\sigma$  and monotonic yield stress  $\sigma_y$ .

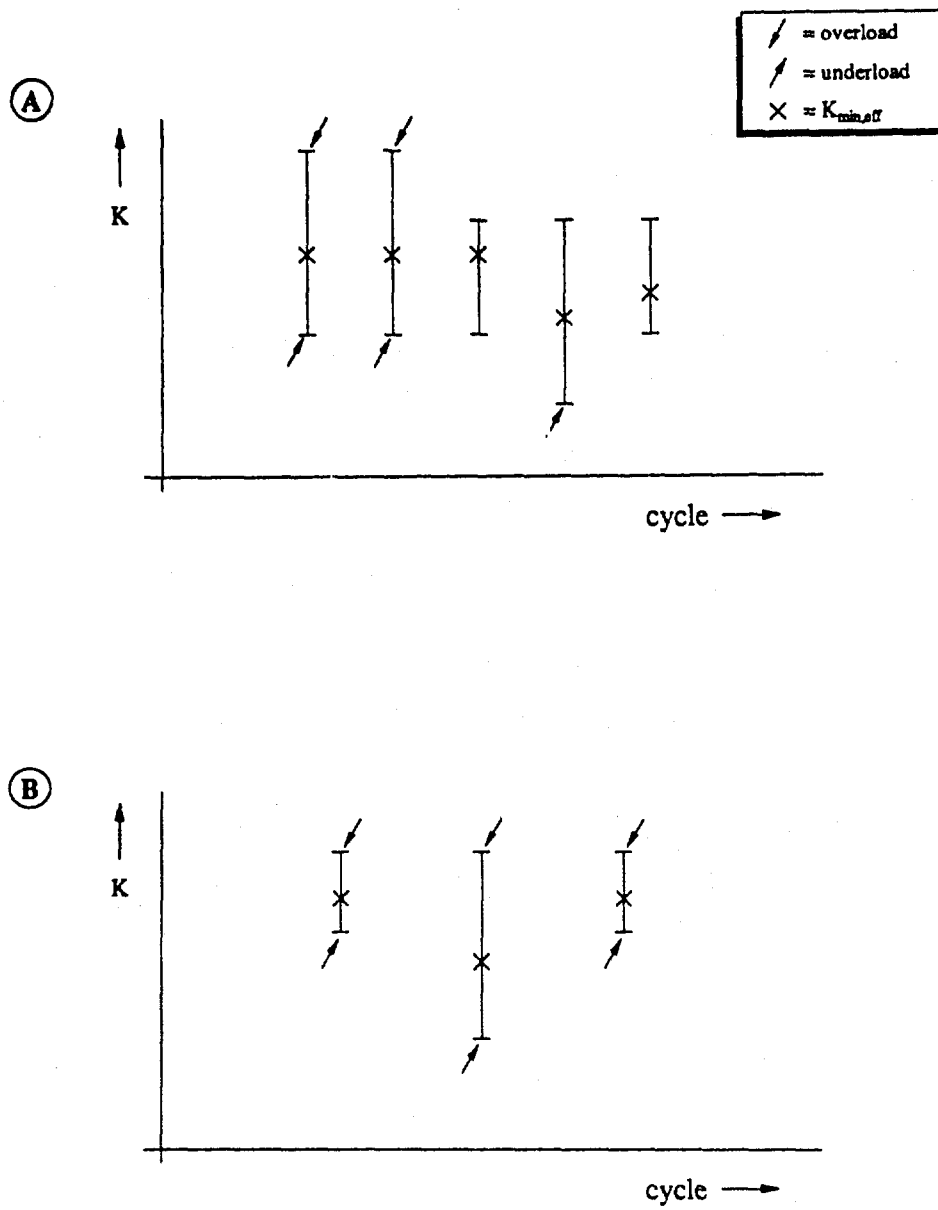
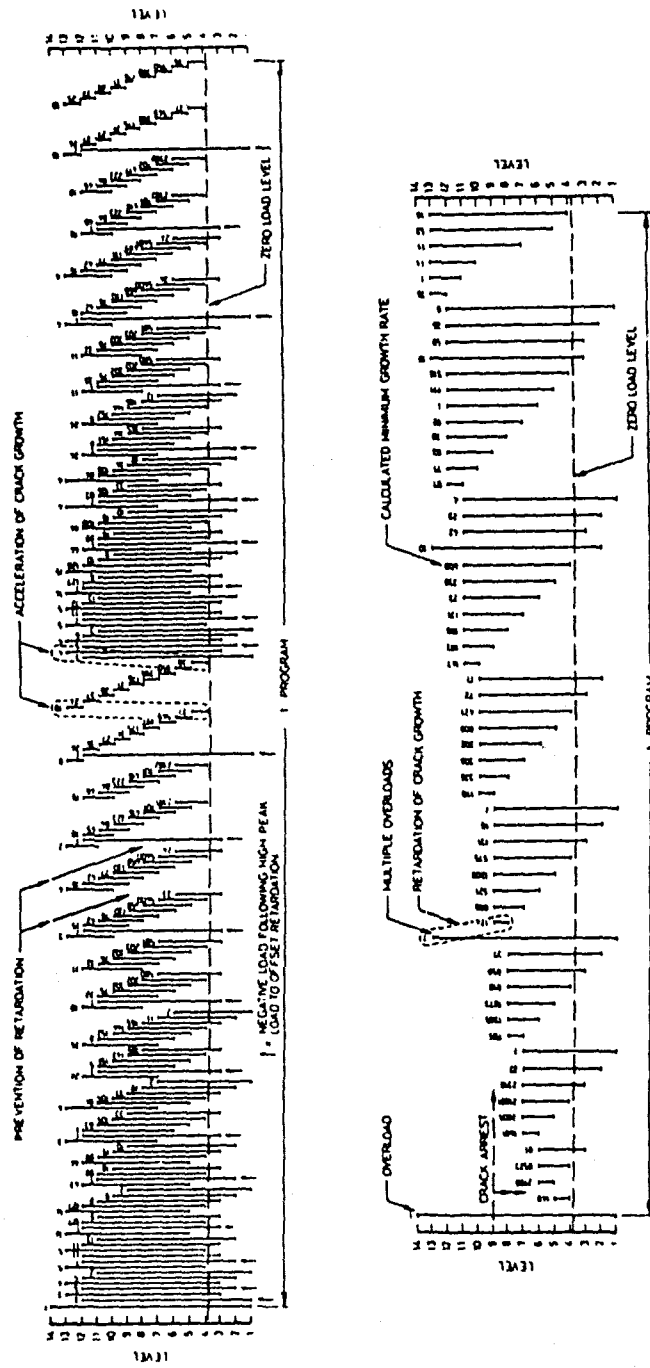


Figure 2.9 Examples of the definition of overloads and underloads.



(a)

(b)

Figure 3.1 The acceleration sequence (a) and the retardation sequence (b).

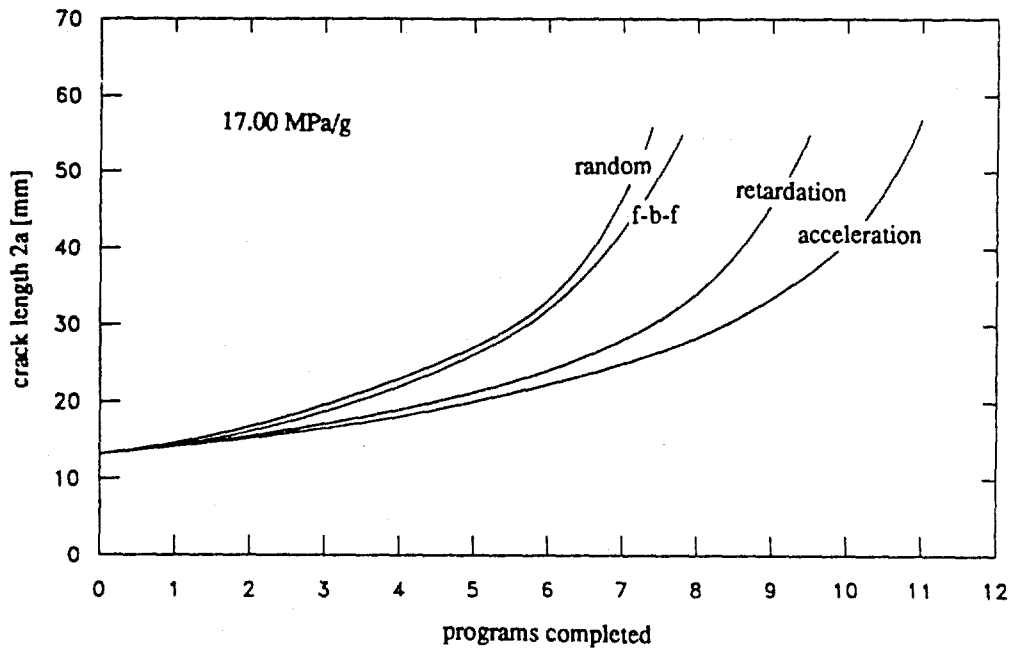
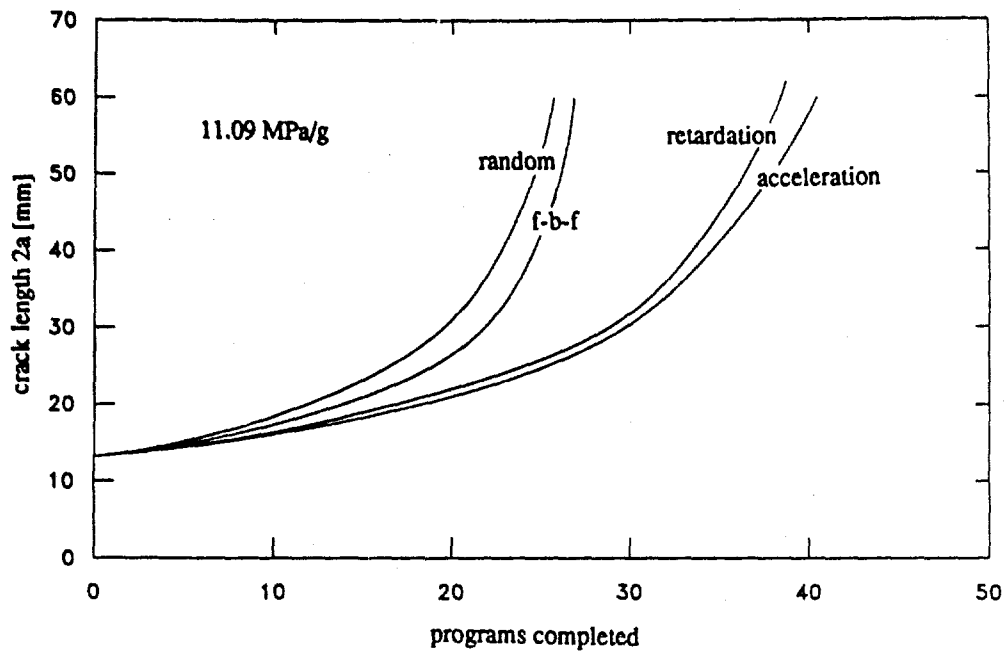


Figure 3.2 Experimental crack growth for the various load sequences and stress levels.

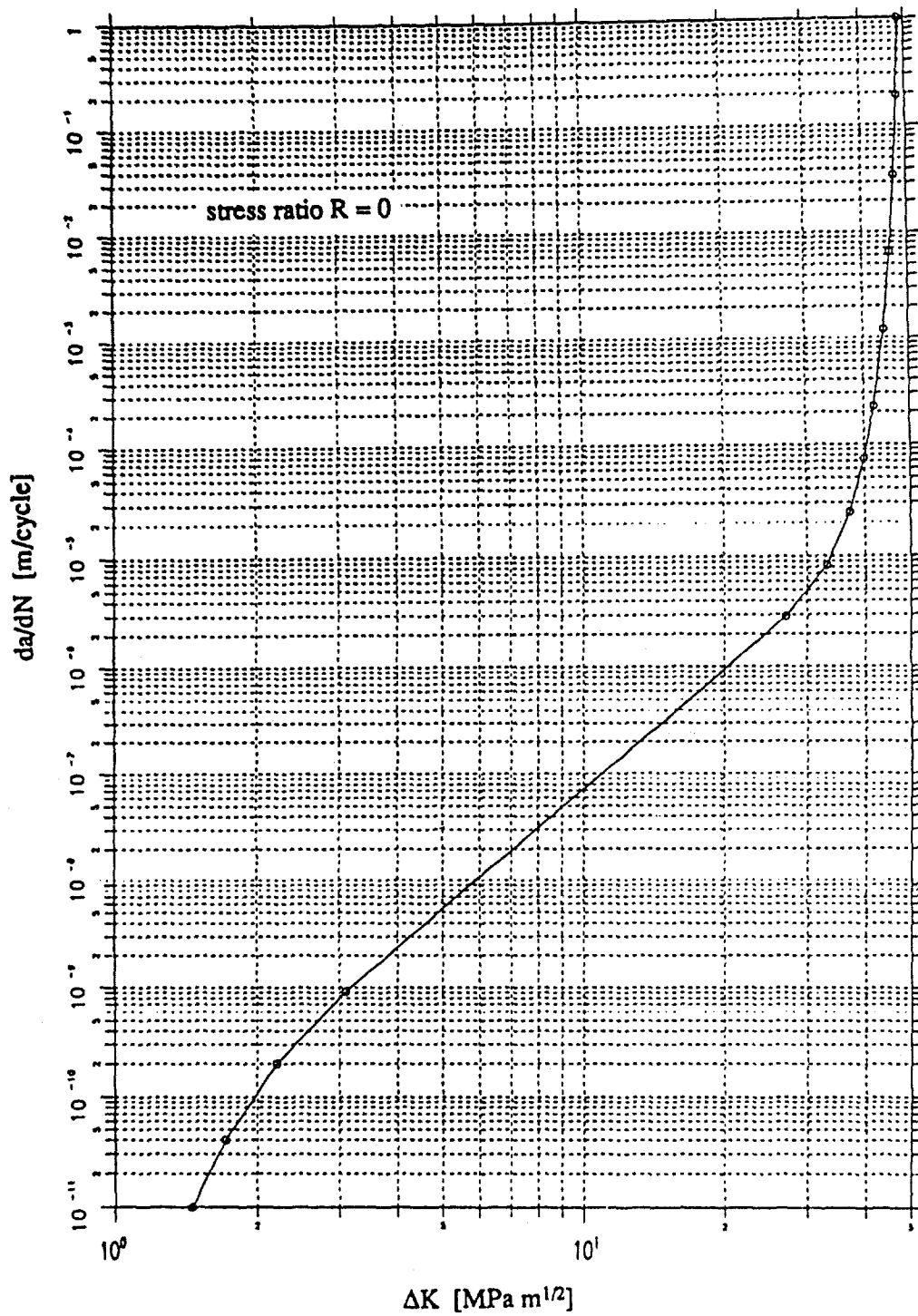


Figure 3.3 Crack growth curve for A7-U4SG-T651 aluminium alloy, stress ratio  $R = 0$ .

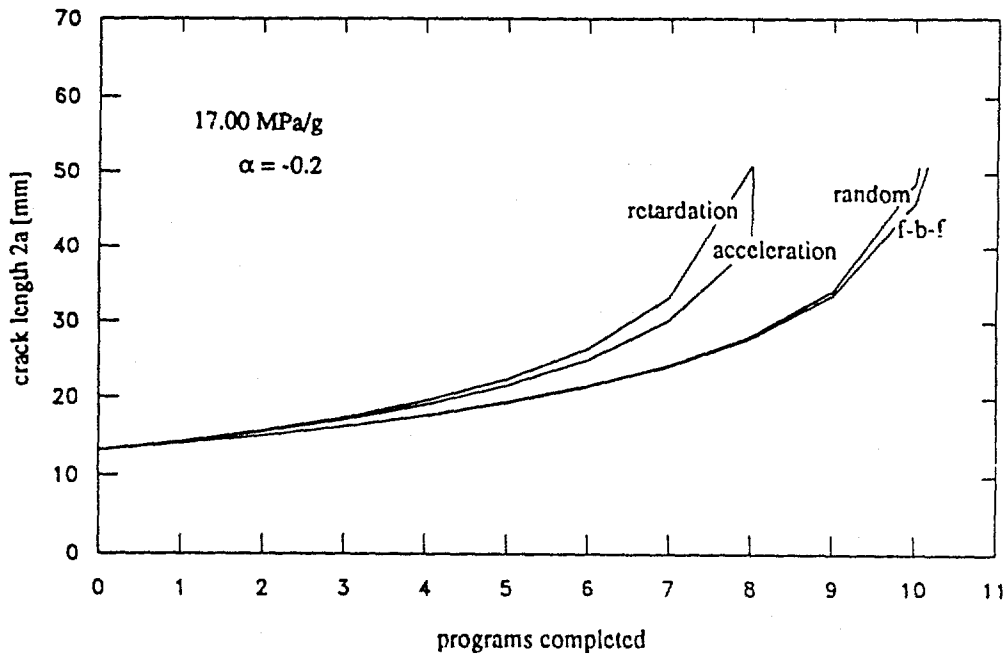
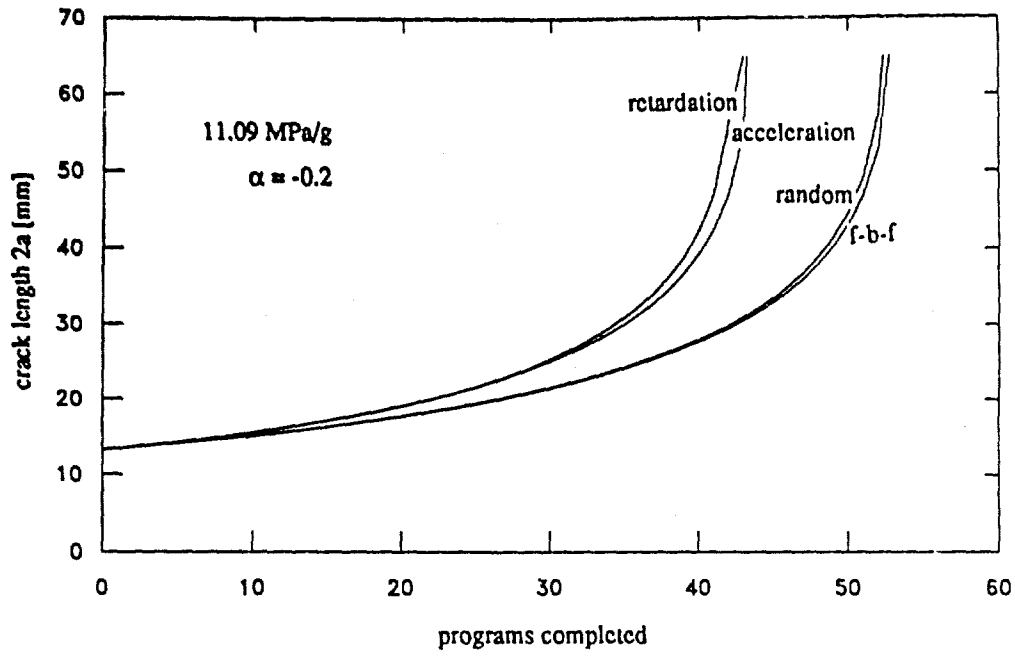


Figure 3.4 Crack growth as calculated with the McAir model for the various load sequences and stress levels ( $\alpha = -0.2$ ).

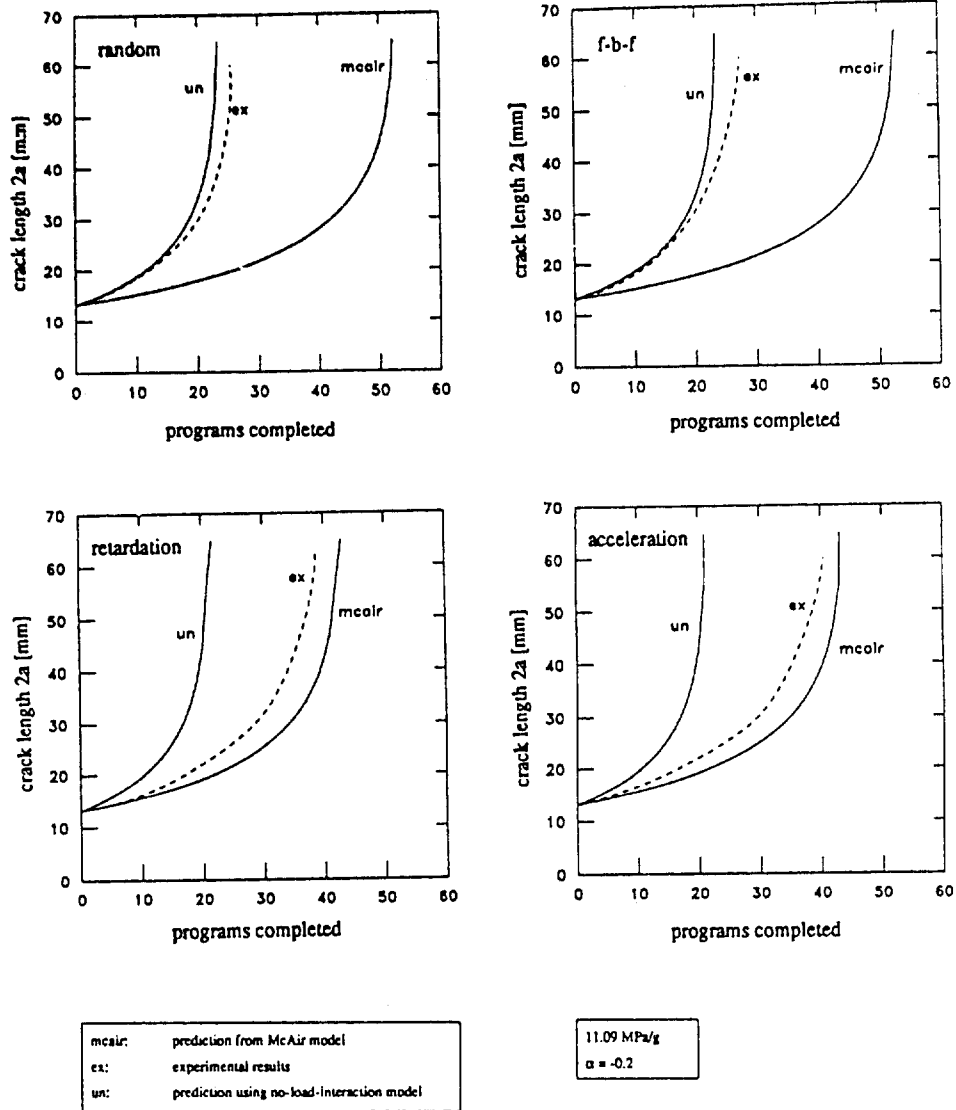


Figure 3.5a Comparison of the predictions from the McAir model ( $\alpha = -0.2$ ) against the experimental results for a stress level of 11.09 MPa/g.

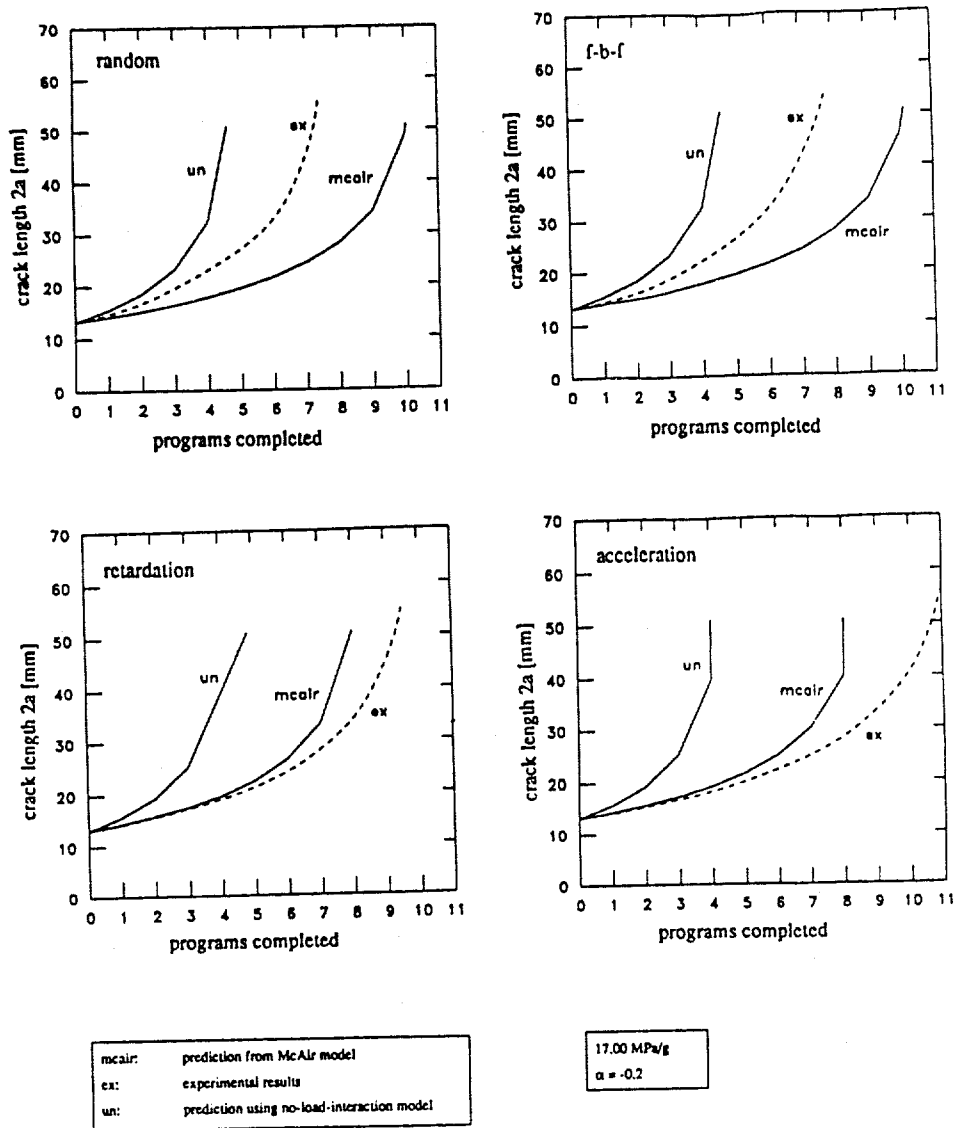


Figure 3.5b Comparison of the predictions from the McAir model ( $\alpha = -0.2$ ) against the experimental results for a stress level of 17.00 MPa/g.

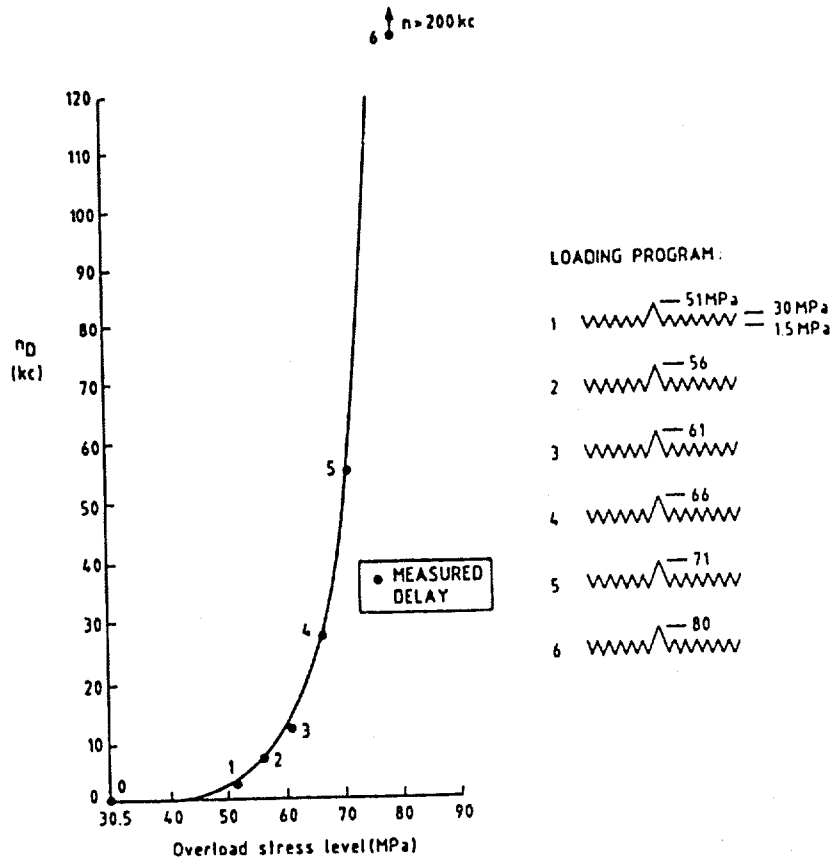


Figure 3.6 Delay period  $N_d$  as a function of the overload level in 7075-T6 aluminium, as found experimentally [15].

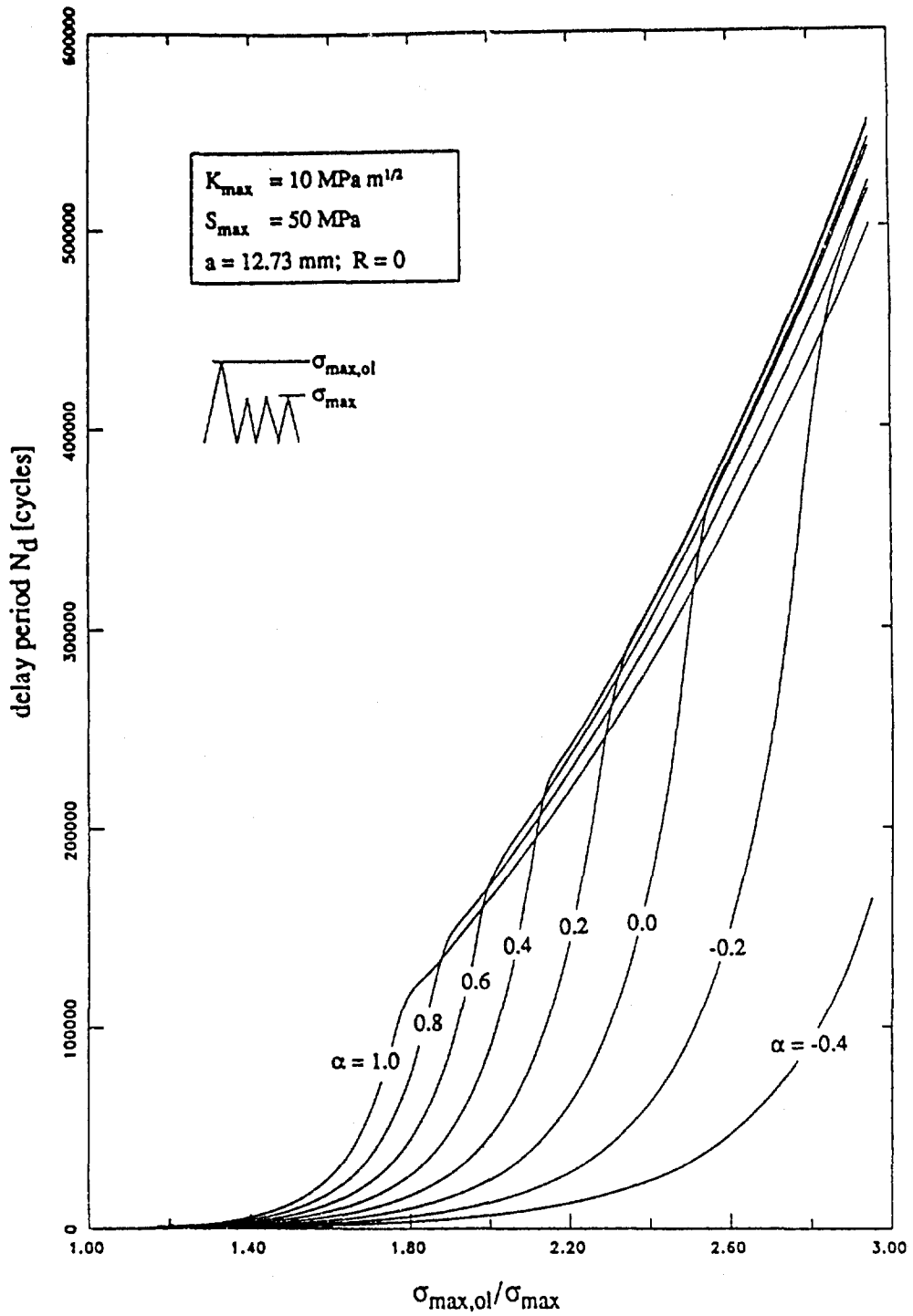


Figure 3.7 Delay period  $N_d$  as a function of the overload level in A7-U4SG-T651 aluminium, as calculated with the McAir model for various values of factor  $\alpha$ .

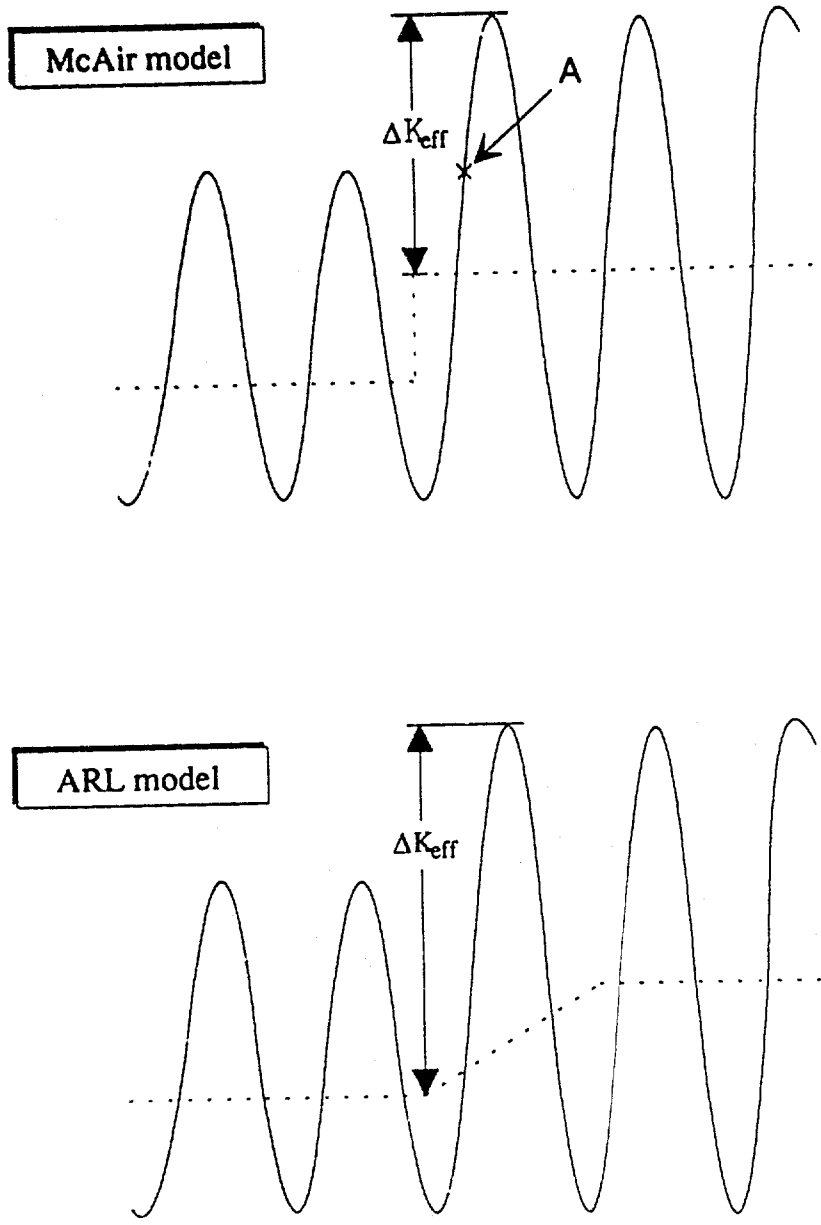


Figure 4.1 Effective stress intensity range for first cycle of block.

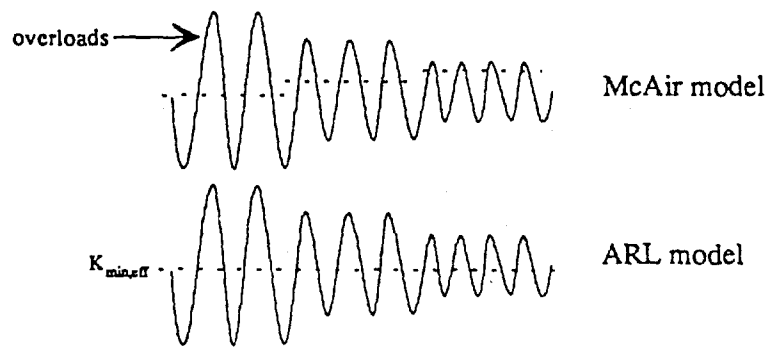
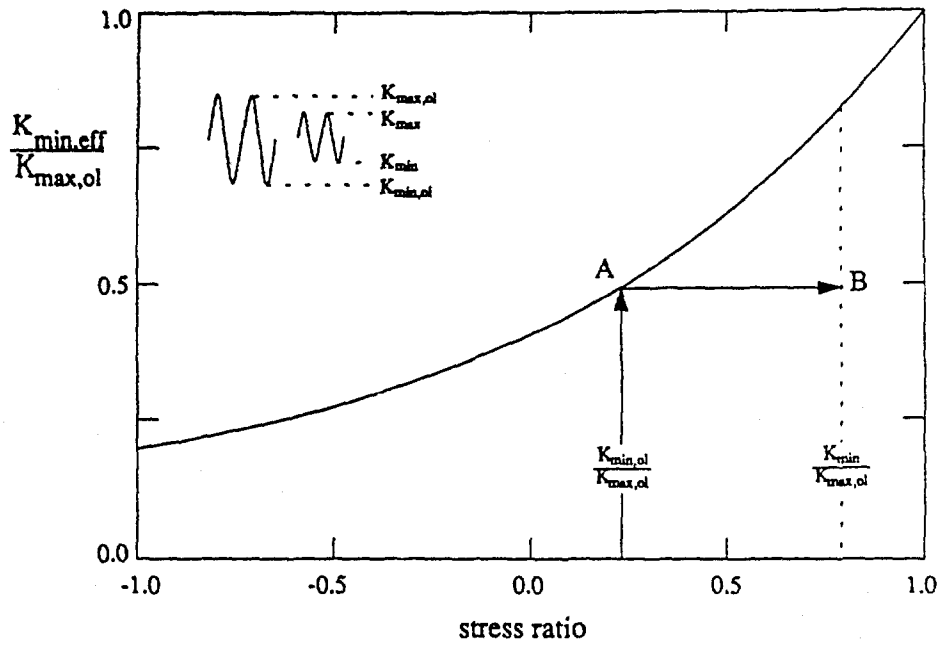


Figure 4.2 Calculation of the minimum effective stress intensity  $K_{min,eff}$  under variable amplitude loading (ARL model).

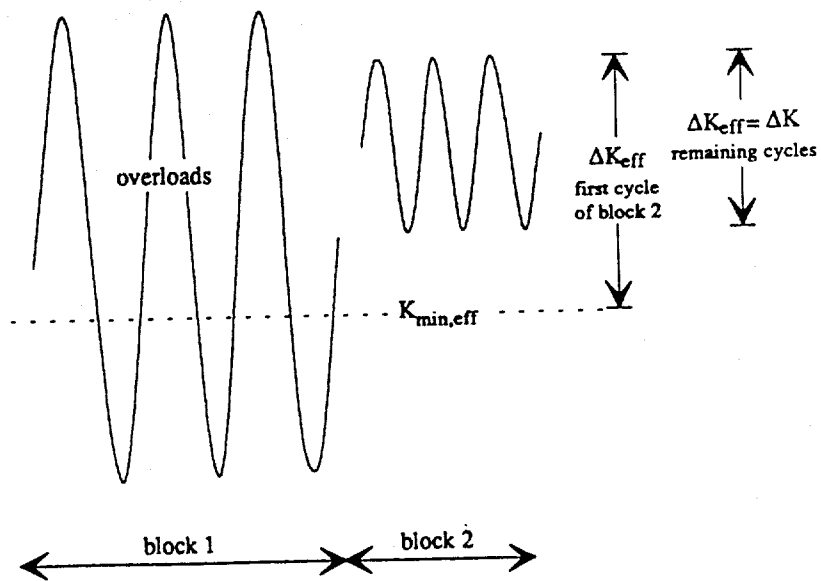


Figure 4.3 The effective stress intensity range  $\Delta K_{eff}$  of the first cycle of a block may be greater than the nominal stress intensity range  $\Delta K$  (ARL model).

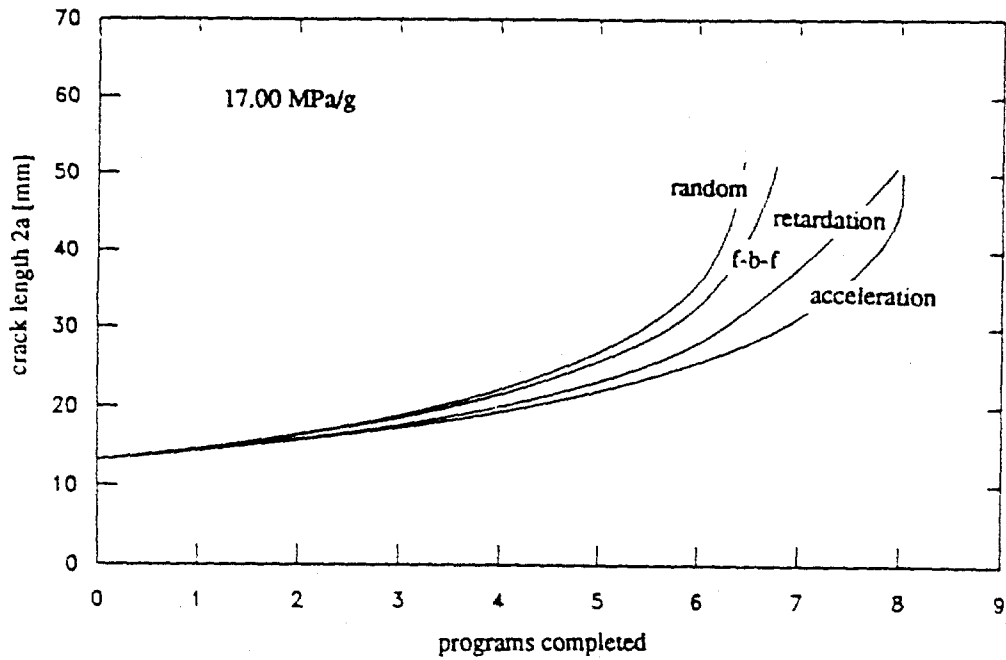
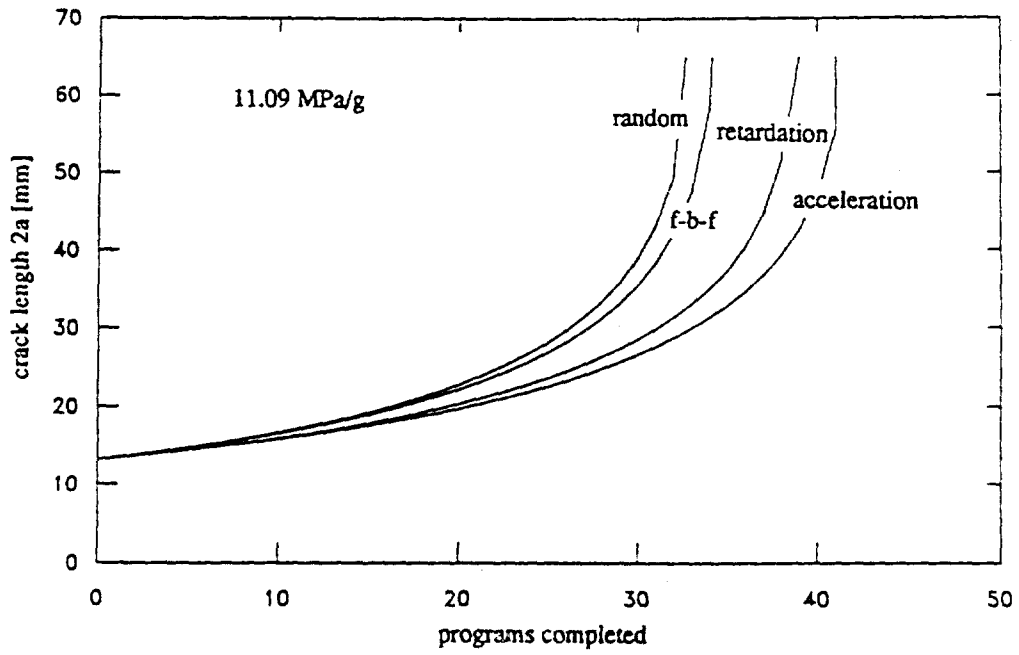


Figure 4.4 Crack growth as calculated with the ARL model for the various load sequences and stress levels.

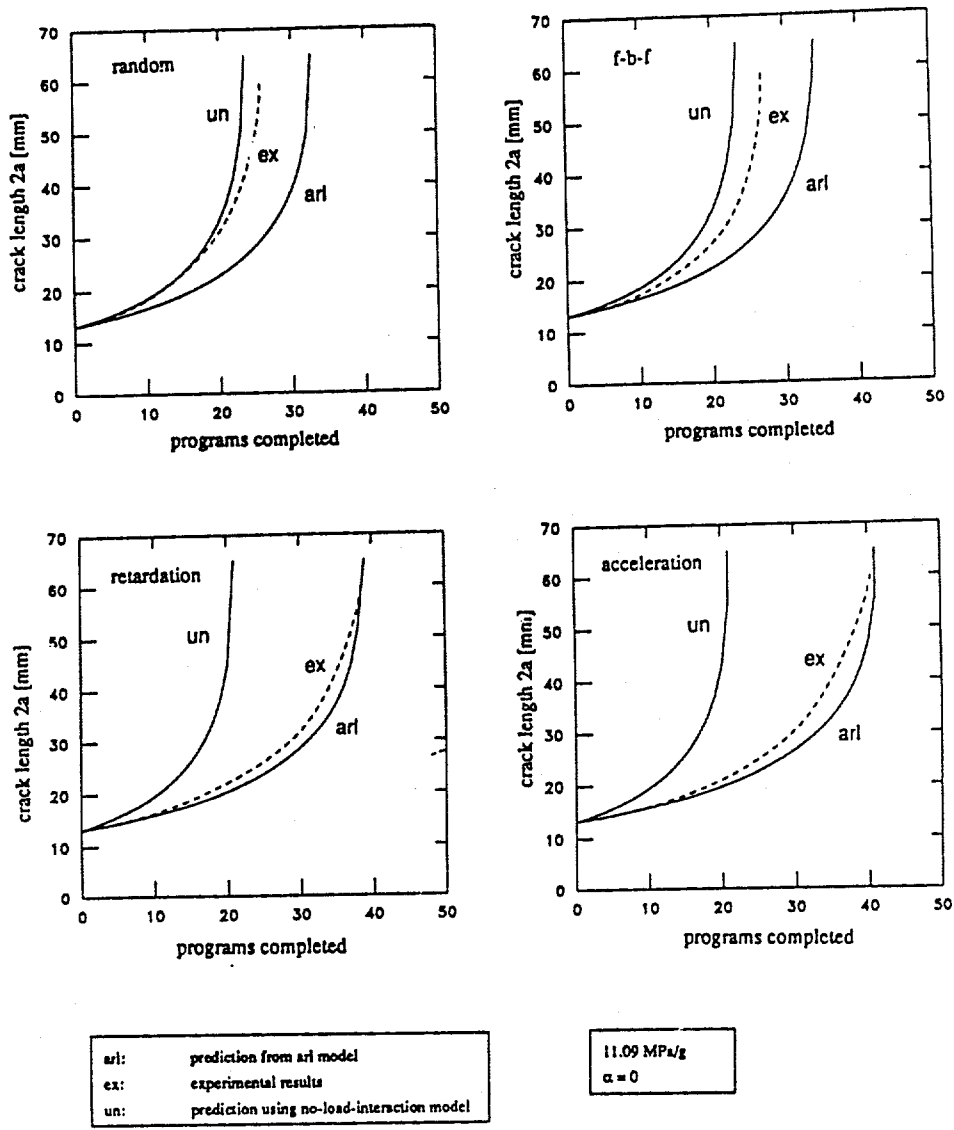


Figure 4.5a Comparison of the predictions from the ARL model against the experimental results for a stress level of 11.09 MPa/g.

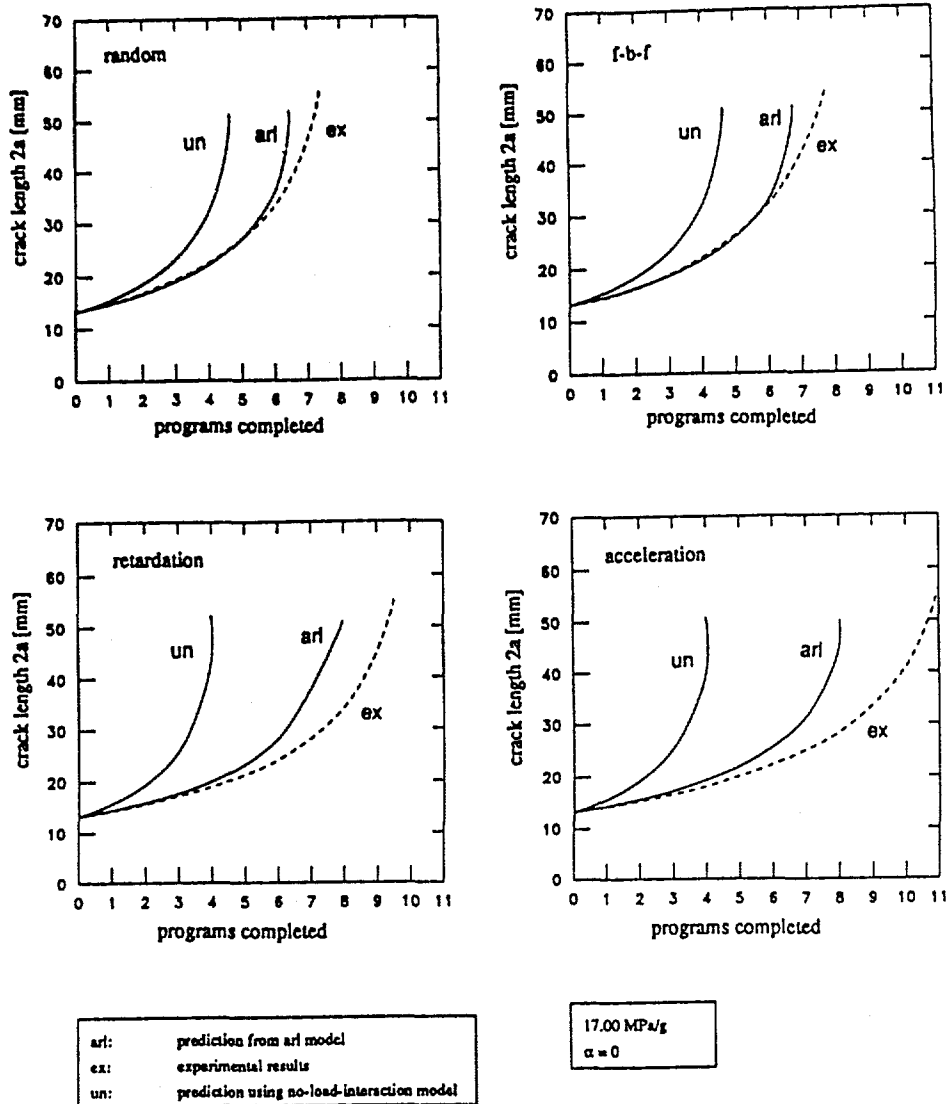


Figure 4.5b Comparison of the predictions from the ARL model against the experimental results for a stress level of 17.00 MPa/g.

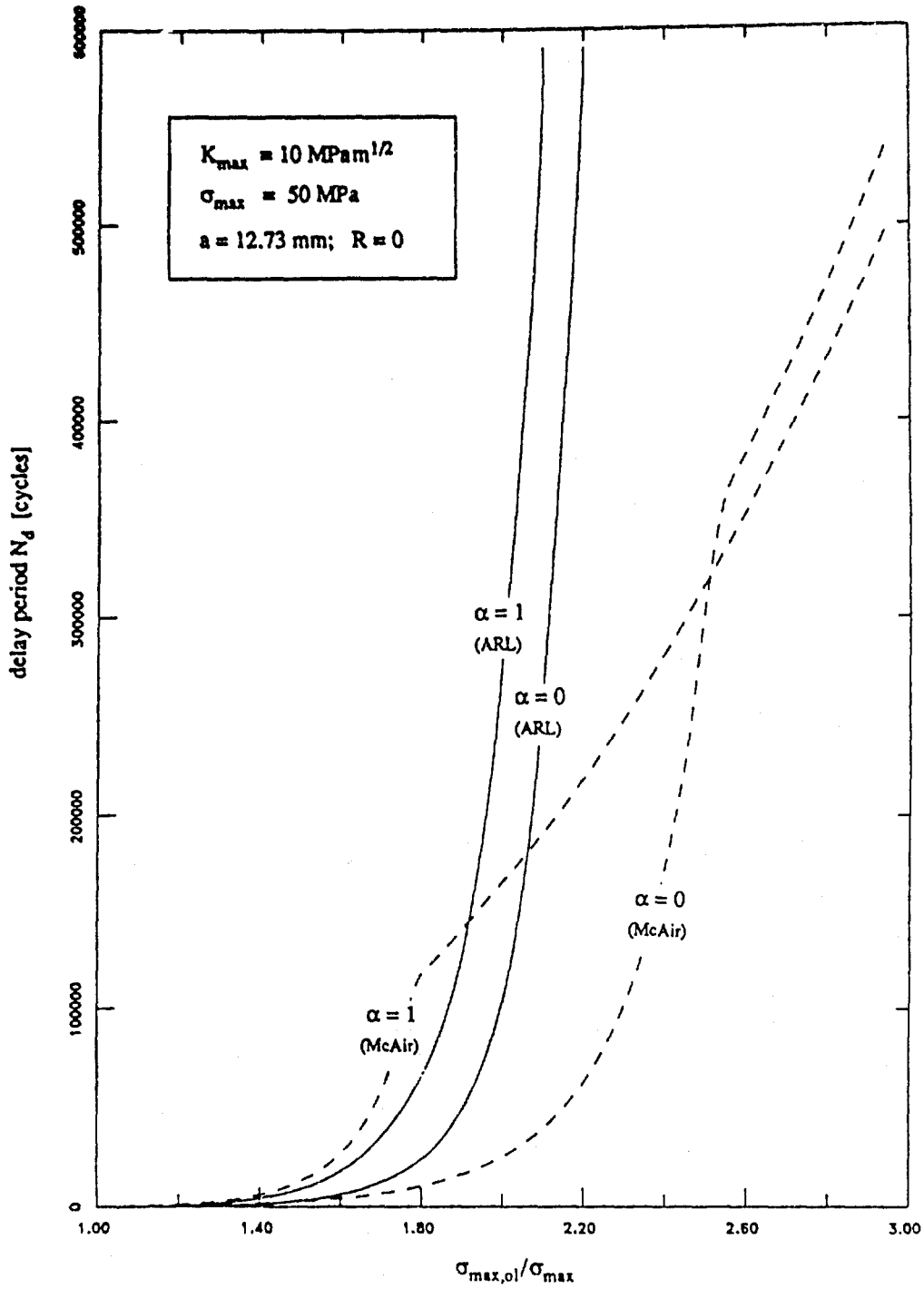


Figure 4.6 Delay period  $N_d$  as a function of the overload level in A7-U4SG-T651 aluminium, as calculated with the ARL model for two values of factor  $\alpha$ .

## APPENDIX A      COMPUTER PROGRAM CNT8SHR

This appendix describes the computer program CNT8SHR. This program incorporates the McAir model as described in this report. It is a stripped version of computer program CNTKM8 that was obtained from McDonnell Douglas. According to a comment in the source listing this latter program dates back to November 1984. It is the latest release available to ARL. Apart from the user's manual the code of CNTKM8 was the only source that provided detailed information on the McAir model. To be able to extract the necessary information it proved useful to rewrite the original source code, since this code had been written in a rather unstructured way. Furthermore the original program covered many options that are not essential for the understanding of the basic McAir model. This finally resulted in computer program CNT8SHR. This program only covers the case of a through crack in a CCT specimen. Care has been taken that the modified version and the original program are fully compatible, so that the same input-files can be used. It has been checked that the same results are obtained for both programs.

The computer program CNT8SHR has been written in Fortran 77. It can be run on a personal computer with a mathematical co-processor. Small jobs with simple load spectra will take up to a few minutes, while in the case of a flight-by-flight spectrum a job may run for more than an hour. The input should be in SI-units without prefixes. The flow diagram of CNT8SHR is given in figure A.1.

### A.1 Interpolation between data points on crack growth curve

Both the original and the modified version of the computer program expect the material's  $R=0$  crack growth curve to be input in tabulated form. The way the two programs interpolate between the data points differs, however. To facilitate interpolation the original program CNTKM8 tries to linearize the  $da/dN$ - $\Delta K$  curve by applying the following transformation to the input data:

$$\begin{aligned} x &= \log(\Delta K_{eff}) \\ y &= \log\left(\frac{K_c \cdot K_{max}}{K_c} \cdot da/dN\right) \end{aligned} \tag{A.1}$$

where  $K_c$  is the material's fracture toughness and  $\Delta K_{eff}$  the effective stress intensity range as calculated with equation (2.1). The transformation of the  $da/dN$ -data is obviously based on Forman's equation for constant amplitude fatigue crack growth. This transformation may seriously affect the accuracy of interpolation, however. This is especially the case when the straight 'Paris-part' of the crack growth curve is represented by the end-points only (which is enough anyway). This can be illustrated with the

following example. Consider the fictitious though realistic  $R=0$  crack growth curve of which the straight part is given by:

$$\log(da/dN) = -31.75 + 3.5\log(\Delta K) \quad (A.2)$$

with  $da/dN$  in m/cycle and  $\Delta K$  in  $\text{Pa}\sqrt{\text{m}}$ . Assuming that  $K_c = 50 \text{ MPa}\sqrt{\text{m}}$  and that  $\Delta K_{\text{eff}}$  is equal to 50% of  $\Delta K$ , this curve could be tabulated as follows:

$\log(\Delta K)$	$\log(da/dN)$	x	y
6.50	-9.00	6.20	-9.028
7.50	-5.50	7.20	-5.935

Now consider a load cycle that results in an effective stress intensity range of  $5 \text{ MPa}\sqrt{\text{m}}$ , while the nominal stress intensity range is  $10 \text{ MPa}\sqrt{\text{m}}$  and  $R=0$ . With equation (A.1) it is found then that  $x = 6.70$  and linear interpolation in the table above yields  $y = -7.482$ . Using equation (A.1) again it is found that the crack growth rate  $da/dN$  is equal to  $4.13 \cdot 10^{-8}$  m/cycle. Using equation (A.2), however, it is found that  $da/dN$  is equal to  $5.62 \cdot 10^{-8}$  m/cycle. It is clear that the latter result is the right one.

The difference between the two  $da/dN$ -values is 36%. It is thus concluded that the Forman-like transformation may suffice for very high  $\Delta K$  values, with  $K_{\text{max}}$  near the fracture toughness, but not for moderate values at all. It was therefore decided not to use this transformation in the modified version CNT8SHR of the original program. It is left to the user to discretize the crack growth curve in such a way that the extremes of the curve are sufficiently accounted for. An example is given in figure 3.3.

It should be noted here that the Forman-like transformation is still applied by the original program CNTKM8. If this program is used this fact should be taken into account. It may be necessary then to increase the number of data points that are used to represent the 'Paris-part' of the crack growth curve.

### A.2 Example problems

The input consists of three data files and a straightforward interactive part. The input should be in SI-units without prefixes, though this is only important in the case of artificially cracked specimens without a load history. In that case no residual plastic zones are present around the crack tip just before cyclic loading starts, and the minimum effective stress intensity in the first cycle is equal to zero. The program, however, always assumes that a plastic zone is present at the time of the first cycle, based on some overload that occurred before analysis starts. Normally this overload is assumed to be equal to the highest load in the input sequence, but for machined slots this overload would be zero. To avoid singularity problems, however, this overload is set to the arbitrary small value of 1000 Pa. This is

---

automatically done by the program. If imperial units (ksi) or SI-units with prefixes (MPa) are used, a value of 1000 is very high, and this is why the input should be in SI-units without prefixes in case of machined slots. If pre-cycled specimens are considered any consistent set of units can be used. It should be noted here that the original program assumes imperial units, although the same argument as above holds.

The three data files to be created are: The *analysis* file, the *material* file and the *spectrum* file. These files will be explained from an example problem. The thick CCT specimen that is considered is made from A7-U4SG-T651 aluminium alloy. The properties of this material are given in tables 1 and 2 of this report. The width equals 100 mm, and the initial machined crack is pre-cycled to a total length of 40 mm. A blocked load program is applied with a maximum gross-area stress, or design limit stress DLS, of 60 MPa. The load program (= spectrum file) consists of 5 blocks of load cycles, and covers 100 flight hours. Two cases will be considered, the first example being straightforward while in the second example a high overload of 120 MPa is applied before starting the fatigue program.

#### A.2.1 Analysis file

The analysis file that covers this example is given in table A.1. It is named *example.anl*. This file contains the information that is not covered by the other files or by the interactive input.

The first line is a commentary line. It can contain up to 72 characters and should not be empty. The second line contains an integer dummy variable. This variable is only used by the original program CNTKM8. The third line contains the specimen width, or twice the shortest distance from the plate edge to the crack centre in case of asymmetric cracks. Lines 4 and 5 contain integer dummy variables that are only used by the original program. The sixth line gives the material file name. The seventh line gives the maximum number of load programs to be analyzed. This is the cut-off for very slow crack growth. The maximum number is 400. This number is determined by the dimensions of the arrays used by the program. The last line contains the number of hours between damage print-out. It is advisable to input a number that is an integer multiple of the number of hours that is covered by the load program.

#### A.2.2 Material file

The material file designates the  $da/dN-\Delta K$  data for use in the analysis. The program transforms the data to a  $da/dN-\Delta K_{eff}$  curve, assuming that the input curve is for a stress ratio of zero. The material file used in this example is given in table A.2, and is named *dadn.dat*.

The first line of the material file is a commentary line. It may contain up to 72 characters and should not be empty. The second line contains Young's modulus, Poisson's ratio, the monotonic yield stress and the cyclic yield stress. It should be noted here that Poisson's ratio actually is a dummy

parameter for CNT8SHR. It is only used by the original program. The third line contains the fracture toughness and the integer number of points in the  $da/dN$ - $\Delta K$  table. This number should not be higher than 50. To avoid singularity problems, the fracture toughness must be slightly higher than the highest  $\Delta K$  that occurs in the table. The remaining lines contain the actual  $da/dN$ - $\Delta K$  table.

### A.2.3 Spectrum file

Spectra (strictly: sequences) may be of any length and form: Random, blocked and flight-by-flight. The stresses are input as a proportion of the design limit stress, which serves as a kind of stress scaling factor. The design limit stress is input manually. In that way it is easy to perform a parametric study involving the stress level. For this example two stress spectra are created. One for the 'regular' case, named *exempl1.seq*, and one for the overload case, named *exempl2.seq*. They are given in tables A.3a and A.3b. The two files are identical, except for the third line.

Again, the first line of the spectrum file is a commentary line. It may contain up to 72 characters and should not be empty. The second line contains the (integer) number of blocks *nlevs* of load cycles in the program, and the number of flight hours that is represented by the program. For random or cycle-by-cycle sequences each block would consist of one cycle.

The third line contains the highest and lowest stress previously experienced, as a proportion of the design limit stress. These stresses are used to initialize  $K_{min,eff}$ . Usually these stresses are equal to the highest and lowest that occur in the sequence. In the case of a machined slit that has not been pre-cycled these stresses must be set to zero. This tells the program that no residual plastic zones are present around the crack tip yet. It is also possible to input a higher stress than present in the program. Effectively this means the application of a high overload just before cycling starts. Comparison of tables A.3a and A.3b shows that in the second example an overload equal to twice the design limit stress is applied, as was required.

The next *nlevs* lines contain the actual load spectrum. Each line contains a block of cycles in the following format: Maximum cyclic stress, minimum cyclic stress, number of cycles in block. Again, the stresses are input as a proportion of the design limit stress. The crack length is assumed to be stationary within a block of cycles. This means that the stress intensity is assumed to be constant during a block. It therefore is advisable to limit the number of cycles within a block to avoid inaccurate answers in case of highly loaded specimens. It may be necessary then to split a block up into two or more parts. The last line contains an integer dummy parameter.

### A.2.4 Interactive input

A few parameters have to be input by hand. This facilitates parametric studies involving these



```

c   ITCYC      total number of cycles that specimen already has      c
c   experienced
c   KK        counter that keeps track of the number of times      c
c   that intermediate results are stored in
c   arrays AI and HI
c   *NBLKS    max. number of spectrum blocks to be analyzed      c
c   *NDADN    number of points in da/dn table (R=0 data)          c
c   *NLEVS    number of load levels in spectrum                    c
c
c   real variables:
c
c   A         current crack length
c   AI(j)     intermediate cracklength, associated with HI(j)     c
c   *Ain      initial crack length in [m]
c   *ALPHA    retardation parameter
c   *AMP      amplification factor, ratio of highest load in
c   magnified inspection interval to highest load
c   in spectrum block
c   AOL      crack length at time of overload
c   BETA     parameter that is derived from ALPHA
c   BETAL    parameter that is derived from ALPHA and XNU
c   *BHRS    number of hours represented by spectrum block
c   CHECK    criterion used to determine if KMAXOL should be
c   updated
c   CODMAX   crack tip opening at time of overload
c   CODX     some crack tip opening
c   CORFAC   correction factor that is applied to K to account
c   for finite width of specimen
c   *CYCLES  number of cycles in block
c   *CYLD    cyclic yield stress in N/m2
c   DADN     actual crack growth da/dn, associated with DKEFF,
c   as found from interpolation in modified material's
c   da/dn vs. delta-K table
c   *DADNB(j) da/dn part of material's da/dn vs. delta-K table
c   for R=0 (j.le.NDADN) in [m/cycle]
c   *DELKB(j) delta-K part of material's da/dn vs. delta-K table;
c   (later on converted into some effective value)
c   DELKB(NDADN) should be less than Kc; in [Pa sqrt(m)]
c   DKEFF    equal to KMXEFF-KMNEFF
c   *DLS     design limit stress in [N/m2]
c   *E       modulus of elasticity in [N/m2]
c   EFFKC    part of equation for KMNEFF
c   EFFKR    if SR=0 then EFFKR = EFFKC/Kmax
c   FR       ratio CYLD/TYLD
c   HI(j)    intermediate result, couples the total number of
c   experienced hours to AI(j)
c   HOURS    equal to #completed blocks*BHRS (before failure)
c   or the time to failure
c   *Kc      material fracture toughness in [Pa sqrt(m)]
c   KMAX     max K in cycle
c   KMAXOL   max K in overload cycle
c   KMIN     min K in cycle
c   KMINOL   underload
c   KMNEFF   effective min. K in cycle
c   KMXEFF   effective max. K in cycle
c   PHOURS   gives the time at which next intermediate results
c   should be printed
c   *PRTHRS  number of spectrum hours between damage printout
c   (must be .GE. BHRS)
c   RC       delta-K/RC gives the effective K for R=0
c   this parameter mainly depends on ALPHA
c   REFK     equal to AMP*SMAX1*CORFAC*DSQRT(PI*A)
c   if REFK exceeds Kc then failure is assumed
c   used in final calculation of A at failure
c   RLFKIA   max stress in cycle
c   *SIGmax  min stress in cycle
c   *SIGmin  either equal to SMAX1 or to 1000. (= small number
c   Smax     if SI-units) if specified spectrum file ISPID
c   Smax1    highest stress in spectrum (or higher if specified
c   in ISPID)
c   Smin     lowest stress in spectrum (or lower), or 0 if
c   Smax = 1000.
c   SR       stress ratio Xmin/Kmax
c   *Tyld    monotonic yield stress in N/m2
c   *W       twice the shortest distance from plate edge to
c   crack center in [m] (width)
c   WOL     plastic zone size due to overload
c   X2      storage for A
c   XALPHA   see equation (2.1) of report
c   XCYC    number of cycles in a spectrum block
c   XFR     see equation (2.1) of report
c   XINCR   used in calculation of A at failure
c   *XNU     Poisson's ratio

```



```

        print *, ' DLS should be greater than 0!'
        print *, ' The program STOPS'
        stop
    END IF

    HI(1) = 0.
    AI(1) = AIN
    A      = 0.

    READ (2,*) W
    READ (2,*) dummy
    READ (2,*) dummy
c    ...used to be npts2 and npts3, resp.

    read (2, '(a)') MATFIL
    read (2, * ) NBLKS
    read (2, * ) PRTHRS

    CLOSE (2)

    OPEN (UNIT=1, FILE=MATFIL, STATUS='OLD')

    read (1, '(a)') TITLE
    read (1, * ) E, XNU, TYLD, CYLD
    read (1, * ) KC, NDADN

    IF (Kc .le. 0.0) THEN
        print *, ' Kc should be greater than 0!'
        print *, ' The program STOPS'
        stop
    END IF

    DO I = 1, NDADN
        READ (1,*) DELKB(I), DADNB(I)
    end do

    CLOSE (1)

c
c
c    READ STRESS EXCEEDANCE DATA...

    ibidx = 'ibid00'
    OPEN (UNIT=3, FILE=IBIDX, STATUS='NEW', FORM='UNFORMATTED')

    read (4, '(a)') TITLE
    read (4, * ) NLEVS, BHRS
    read (4, * ) SMAX, SMIN

    IF (SMAX.LT..01) IFLAG = 1

    SMAX = SMAX*DLS
    SMIN = SMIN*DLS

    DO I = 1, NLEVS
        READ (4,*) SIGMAX, SIGMIN, CYCLES
        XCYC = XCYC+CYCLES
        SIGMAX = SIGMAX*DLS
        SIGMIN = SIGMIN*DLS
        IF (SIGMAX.GT.SMAX) SMAX = SIGMAX
        IF (SIGMIN.LT.SMIN) SMIN = SIGMIN
        WRITE (3) SIGMAX, SIGMIN, CYCLES
    end do

    READ (4,*) dummy
c    ...used to be num

    CLOSE (4)
    CLOSE (3)

    OPEN (UNIT=3, FILE=IBIDX, STATUS='OLD', FORM='UNFORMATTED')

    SMAX1 = SMAX
    IF (IFLAG.EQ.1) THEN
c        if SI-units then...
        SMAX = 1000.
c        else smax should be +/- 0.001
        SMIN = 0.
    END IF

c
c
c    COMPUTE CONSTANT MODEL PARAMETERS

    BETA = ALPHA*(1.-ALPHA)/2.
    BETA1 = ALPHA*(1.-ALPHA)*(1.-XNU**2)/2.

```



```

                WOL = PI/8.*BETA*(KMAXOL/YLD1)**2
                CODMAX = BETA1*KMAXOL**2/2./E/YLD1
                AOL = A
            end if
        end if

        IF (KMIN.le.KMINOL) then
            KMINOL = KMIN
            SR = KMINOL/KMAXOL
            XR = 0.46733+0.29401*SR+0.23866*SR**2
            XALPHA = 1.-(1.-DSORT(BETA))*(1.-SR)
            XFR = 1.-(0.756-0.912*FR+0.156*FR**2)*(1.-SR)
            EFFKC = XR*XALPHA*XFR*KMAXOL - 0.225*KMINOL
            IF (SR.LT.0.) EFFKC = EFFKR*KMAXOL*DEXP(0.08*SR)
        end if

        REFK = AMP*SMAX1*CORFAC
        IF (REFK .ge. KC) GOTO 210

C
C
        COMPUTE EFFECTIVE KMIN AND DELTA K
C
        IF (KMAX .le. 0.) THEN
            ...da/dn = 0
            X2 = A
        ELSE
            KMXEFF = EFFKC+0.225*KMAX
            IF (KMXEFF.LT.KMAX) KMXEFF = KMAX
            IF (KMXEFF.LT.0.) KMXEFF = 0.

            IF (KMAX.GE.KC) THEN
                PRINT *, 'KMAX EXCEEDED KC', KMAX
                GOTO 210
            END IF

            KMNEFF = EFFKC+0.225*KMIN
            IF (KMNEFF.LT.0.) KMNEFF = 0.
            IF (KMNEFF.LT.KMIN) KMNEFF = KMIN
            DKEFF = KMXEFF-KMNEFF

C
C
            IF KMAX IS LESS THAN KMNEFF GROWTH IS ZERO...
C
            IF (DKEFF.gt.0.) THEN
                COMPUTE DA/DN AND CRACK GROWTH...

                DKEFF = DLOG10(DKEFF)
                CALL TLU(DELKB,DADNB,NDADN,DKEFF,DADN)
                old: DADN = 10.**DADN*KC/(KC-KMAX)
                dadn = 10.**dadn
                X2 = A
                A = A + DADN*CYCLES

                IF (A .ge. W/2) THEN
                    REFK = AMP*SMAX1*CORFAC
                    PRINT *, 'THE CRACK LENGTH IS EXCEEDING THE WIDTH'
                    PRINT *, 'HOURS = ', HOURS
                    PRINT *, 'LI/2 = ', A
                    PRINT *, 'REFK = ', REFK
                    GOTO 250
                END IF
            END IF
        END IF

200 CONTINUE

C
C
        CHECK THAT KC HAS NOT BEEN EXCEEDED...
C
        IF (REFK.GT..95*KC) THEN
            CALL KCOR(a,w,CORFAC)
            REFK = AMP*SMAX1*CORFAC*DSQRT(PI*A)
        END IF
        IF (REFK .lt. KC) GOTO 225

210 XONE = X2

        DO J = 3,7

C
            Initialize...
            XINCR = 1./(10.**J)
            REFKIA = Kc - 1.
            II = 1

```

```

DO while ((REFKIA.le.Kc) .and. (II.le.100))
  A = XONE+II*XINCR

  if (a .ge. w/2) then
    REFK = AMP*SMAX1*CORFAC
    PRINT *, 'THE CRACK LENGTH IS EXCEEDING THE WIDTH'
    PRINT *, 'HOURS = ', HOURS
    PRINT *, 'LI/2 = ', A
    PRINT *, 'REFK = ', REFK
    GOTO 250
  end if

  CALL KCOR(a,w,CORFAC)
  CORFAC = CORFAC*DSQRT(PI*A)
  REFKIA = AMP*SMAX1*CORFAC
  II = II+1
END DO

IF (II.GE.100) THEN
  PRINT *, 'PROBLEMS WITH ACRR ITERATIONS'
  STOP
ELSE
  XONE = A-XINCR
END IF
END DO

IF (M.EQ.1 .AND. N.EQ.1) THEN
  PRINT *, 'FAILED IMMEDIATELY'
  IFALL = 1
  GOTO 250
END IF

HOURS = BHRS*(M-1+((YCYC-CYCLES)/XCYC))
REFK = REFKIA

WRITE (6,320)
WRITE (6,350) HOURS,A,REFK

GOTO 250

      (OUTPUT RESULTS)

225  HOURS = BHRS*M

      IF (HOURS.ge.PHOURS) then
        PHOURS = PHOURS+PRTHRS
        WRITE (6,350) HOURS,A,REFK
        KK = KK+1
        HI(KK) = HOURS
        AI(KK) = A
      end if

      REWIND 3
      YCYC = 0.

      END DO

250 IF (IFALL.ne.1) then
      KK = KK+1
      HI(KK) = HOURS
      AI(KK) = A
    end if

      CLOSE (3,STATUS='DELETE')

888 write (*,'(lx,a,$)') 'Enter the name of your PREDICTION file: '
      read (*,'( a )') ipred
      open (unit=1, file=ipred, status='new', err=888)

      write (1,'(lx,a/)') ' INPUT DATA'
      write (1,'(lx,a/)') ' titles
      write (1,'(lx,a/lx.a/)') 'No FORMAN-transformation of dadn-curve',
+ 'and YLD1 calculated outside if-block'
      write (1,'(lx,a, lx,a )') 'Analysis data: file =', iafid
      write (1,'(lx,a, F7.3 )') ' ALPHA =', alpha
      write (1,'(lx,a,E13.5 )') ' Ain =', ain
      write (1,'(lx,a,E13.5 )') ' W =', w
      write (1,'(lx,a,E13.5 )') ' DLS =', DLS
      write (1,'(lx,a, F7.3/)') ' AMP =', amp

```

```

write (1, '(lx,a, lx,a )') 'Material data:  file =', matfil
write (1, '(lx,a,E11.3 )') '              E =', E
write (1, '(lx,a, F7.3 )') '              Xnu =', xnu
write (1, '(lx,a,E11.3 )') '              Tyld =', tyld
write (1, '(lx,a, F7.3 )') '              FR =', FR
write (1, '(lx,a,E11.3/)' ) '              Kc =', KC

write (1, '(lx,a, lx,a )') 'Spectrum data:  file =', isfid
write (1, '(lx,a, i7 )') '              Nlevs =', nlevs
write (1, '(lx,a,E11.3 )') '              Bhrs =', bhrs
write (1, '(lx,a,E11.3/)' ) '              Smax1 =', smax1

write (1, '(/lx,a/)' ) '              OUTPUT DATA'

IF (IFAL1.ne.1) then
  WRITE (1,997) M,ITCYC,N,HOURS
  WRITE (1,996) A,REFK
  WRITE (1,995) SIGMAX,SIGMIN,CYCLES
end if

write (1, '(/lx,a/)' ) '              Hours              A'
do i = 1,KK
  write (1, '(lx,F14.3,F15.6)' ) HI(i),AI(i)
end do

CLOSE (1)

STOP 1776

280 FORMAT( / ' CONTACT STRESS MODEL-III ANALYSIS' /)
320 FORMAT(/2X,'STRESS INTENSITY EXCEEDED IN A DIRECTION :'/)
339 FORMAT(/' BEGIN SPECTRUM CRACK GROWTH ANALYSIS, A =',E12.5
+//T8,'HOURS',T22,'A',T29,' KREFERENCE'/)
350 FORMAT(' ',F11.0,F15.9,F12.1)
997 FORMAT( 5X,'BLOCKS  =',I8,/5X,'TOT.CYC =',I8,/5X,'LAYER  =',I8,
+ /5X,'HOURS  =',F9.0)
996 FORMAT(5X,'A      =',F9.6,/5X,'KREFA  =',e11.4,/5X)
995 FORMAT(5X,'SIGMAX =',e11.4,/5X,'SIGMIN =',e11.4,/5X,'CYCLES =',
+ ,F10.0,/)

E N D

SUBROUTINE KCOR(a,w,CORFAC)
IMPLICIT REAL*8 (A-H,O-Z)
DATA PI/3.1415926536/
CORFAC = DSQRT(1./dcos(pi*a/w))
RETURN
E N D

SUBROUTINE TLU(X,Y,N,XVAL,YVAL)
IMPLICIT REAL*8 (A-H,O-Z)
DIMENSION X(N),Y(N)
IF(X(N).GE.XVAL) GO TO 10
I = N
GO TO 30
10 DO 20 I = 1,N
  IF(X(I).GE.XVAL) GO TO 30
20 CONTINUE
30 IF (I.EQ.1) I = 2
  YVAL = (Y(I)-Y(I-1))/(X(I)-X(I-1))*(XVAL-X(I-1))+Y(I-1)
RETURN
E N D

```

```

Example problem
4
.1
0
0
dadn.dat
400
100.

```

Table A.1 Example analysis file, named *example.anl*.

```

Material's curve for A7-U4SG-T651 in [N,m]
6.90e10 .3 457.e6 .411.e6
4.90e7 14
1454550. 1.000000E-011
1711900. 4.000000E-011
2201980. 1.993473E-010
3097420. 9.201416E-010
2.69774E+007 2.864725E-006
3.30770E+007 8.310194E-006
3.70996E+007 2.461269E-005
3.99125E+007 7.389003E-005
4.19771E+007 2.238263E-004
4.42058E+007 1.193590E-003
4.57876E+007 6.425438E-003
4.69660E+007 3.481965E-002
4.78767E+007 1.896133E-001
4.86000E+007 1.0

```

Table A.2 Example material file, named *dadn.dat*.

```

Example spectrum file (1)
5 100.
1.00 -0.20
1.00 0.05 1000.
0.40 -0.10 5000.
0.60 0.00 3000.
1.00 0.40 2000.
0.50 -0.20 3500.
0

```

Table A.3a First example spectrum file, named *exampl1.seq*.

```

Example spectrum file (2)
5 100.
2.00 -0.20
1.00 0.05 1000.
0.40 -0.10 5000.
0.60 0.00 3000.
1.00 0.40 2000.
0.50 -0.20 3500.
0

```

Table A.3b Second example spectrum file, named *exampl2.seq*.

Modified version of the McAir crack growth program CNTKM8.  
No Forman-transformation of the da/dn-curve

Marcel Bos, 5/3/91.

WARNING: In case of pre-cycled specimens it does not matter whether SI-units or Imperial units are used, as long as the input is consistent. In case of saw-cut specimens (line 3 of spectrum file: 0,0) only SI-units should be used however, although the error that is introduced when using imperial units most likely is very small.

Input ANALYSIS file: *example.anl*

Input SPECTRUM file: *examp11.seq*

CONTACT STRESS MODEL-III ANALYSIS

Example problem

Input ALPHA: *0*

AINITIAL: *.02*

DLS: *60e6*

AMP FACTOR: *1*

BEGIN SPECTRUM CRACK GROWTH ANALYSIS, A = .20000E-01

HOURS	A	KREFERENCE
100.	.021410967	17438515.0
200.	.023101030	18484567.7
300.	.025263967	19895103.3
400.	.028267137	22023761.4
500.	.033275489	26150467.9

STRESS INTENSITY EXCEEDED IN A DIRECTION :

576. .043440339 49000029.5

Enter the name of your PREDICTION file: *pred1*

Return code 1776

Table A.4a Interactive input of first example. User's input written in *italic*.

Modified version of the McAir crack growth program CNTKMB.  
No Forman-transformation of the da/dn-curve  
Marcel Bos, 5/3/91.

WARNING: In case of pre-cycled specimens it does not matter whether SI-units or Imperial units are used, as long the input is consistent. In case of saw-cut specimens (line 3 of spectrum file: 0,0) only SI-units should be used however, although the error that is introduced when using imperial units most likely is very small.

Input ANALYSIS file: *example.anl*

Input SPECTRUM file: *examp12.seq*

CONTACT STRESS MODEL-III ANALYSIS

Example problem

Input ALPHA: *0*

AINITIAL: *.02*

DLS: *60e6*

AMP FACTOR: *5*

BEGIN SPECTRUM CRACK GROWTH ANALYSIS, A = .20000E-01

HOURS	A	KREFERENCE
100.	.020103570	16779813.0
200.	.020212387	16846233.6
300.	.020325504	16915458.4
400.	.020443242	16987709.7
500.	.020565959	17063236.6
600.	.022061815	17836254.6
700.	.023919250	19007745.9
800.	.026362594	20648494.6
900.	.029945952	23318507.4
1000.	.037060907	29836113.9

STRESS INTENSITY EXCEEDED IN A DIRECTION :

1007.	.043440407	49000320.5
-------	------------	------------

Enter the name of your PREDICTION file: *pred2*

Return code 1776

Table A.4b Interactive input of second example. User's input written in *italic*.

### INPUT DATA

#### Example problem

No FORMAN-transformation of dadn-curve  
and YLD1 calculated outside if-block

Analysis data: file = example.anl  
ALPHA = .000  
Ain = .20000E-01  
W = .10000E+00  
DLS = .60000E+08  
AMP = 1.000

Material data: file = dadn.dat  
E = .690E+11  
Xnu = .300  
Tyld = .457E+09  
FR = .899  
Kc = .490E+08

Spectrum data: file = exampl1.seq  
Nlevs = 5  
Bhrs = .100E+03  
Smax1 = .600E+08

### OUTPUT DATA

BLOCKS = 6 \*)  
TOT.CYC = 87000  
LAYER = 5 \*)  
HOURS = 576.  
A = .043440  
KREFA = .4900E+08  
SIGMAX = .3000E+08  
SIGMIN = -.1200E+08  
CYCLES = 3500.

Hours	A
.000	.020000
100.000	.021411
200.000	.023101
300.000	.025264
400.000	.028267
500.000	.033275
575.862	.043440

\*) 'Layer' is the McAir denotation for 'block' as used in this report, while 'block' in McAir jargon denotes 'sequence' or 'program'.

Table A.5a Prediction file of first example, named *pred1*.

INPUT DATA

Example problem

No FORMAN-transformation of dadn-curve  
and YLD1 calculated outside if-block

Analysis data: file = example.anl  
ALPHA = .000  
Ain = .20000E-01  
W = .10000E+00  
DLS = .60000E+08  
AMP = .500

Material data: file = dadn.dat  
E = .690E+11  
Xnu = .300  
Tyld = .457E+09  
FR = .899  
Kc = .490E+08

Spectrum data: file = exampl2.seq  
Nlevs = 5  
Bhrs = .100E+03  
Smaxl = .120E+09

OUTPUT DATA

BLOCKS = 11  
TOT.CYC = 151000  
LAYER = 2  
HOURS = 1007.  
A = .043440  
KREFA = .4900E+08

SIGMAX = .2400E+08  
SIGMIN = -.6000E+07  
CYCLES = 5000.

Hours	A
.000	.020000
100.000	.020104
200.000	.020212
300.000	.020326
400.000	.020443
500.000	.020566
600.000	.022062
700.000	.023919
800.000	.026363
900.000	.029946
1000.000	.037061
1006.897	.043440

Table A.5b Prediction file of second example, named *pred2*.

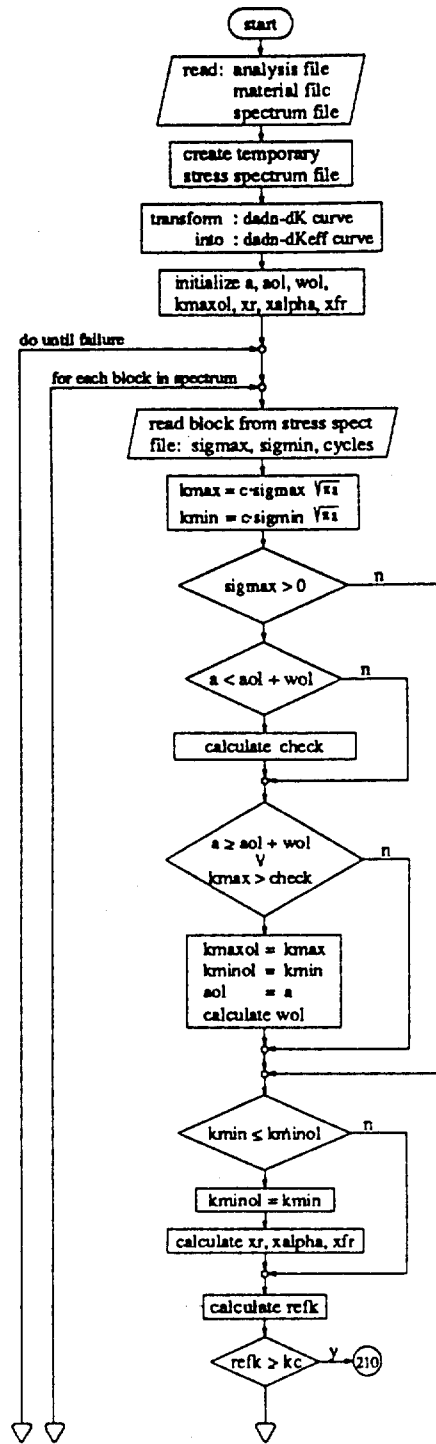


Figure A.1 Flow diagram of computer program CNT8SHR.

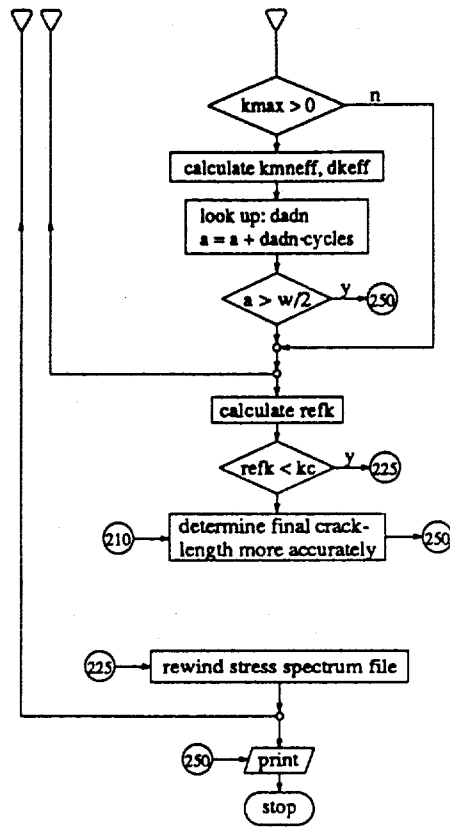


Figure A.1 (continued)

---

## APPENDIX B    COMPUTER PROGRAM ARLECC

In this appendix the source code of computer program ARLECC is listed. This program incorporates the crack closure model as proposed in chapter 4 of this report. It is used for the calculation of the crack growth life of CCT specimens with through cracks. It has been written in Fortran 77, and it can be run on a personal computer with a mathematical co-processor. Although the same spectrum files can be used as for program CNT8SHR, even small jobs with simple blocked spectra may take more than an hour, depending on the applied stress levels. This is due to the fact that ARLECC treats cycles individually, allowing the crack to grow each cycle, whereas CNT8SHR operates on the load blocks as a whole, although it is possible to perform a cycle-by-cycle calculation with the latter program by assigning only one load cycle per block. Unlike CNT8SHR, computer program ARLECC always assumes that the initial crack has experienced prior growth, so that residual plastic zones are present around the crack tip. Computer program ARLECC can also be used to perform 'no-load-interaction analyses', in which case only the stress ratio effect is accounted for, and previous load history is ignored. Any consistent set of units can be used for the input data.

### B.1 Program input

The input consists of two input files and an interactive part. The two input files are the *material* file and the *spectrum* file. They are identical to the ones needed for computer program CNT8SHR. Details can be found in appendix A. Again, a crack growth curve for a stress ratio of zero is expected. The interactive part is very straightforward. Successively the program asks for: The name of the spectrum file, the name of the material file, the value of retardation parameter  $\alpha$ , the initial half crack length, the specimen width, the design limit stress, the amplification factor, and the maximum number of programs to be analyzed. All these parameters, including  $\alpha$ , are similar to the ones described in appendix A. To perform a 'no-load-interaction' analysis a value of -999 must be input for  $\alpha$ . In all other cases a value of between -1 and +1 must be used.

Table B.1 shows what the screen looks like when running the first example of appendix A. Again the data files of tables A.2 and A.3a are used. The output file *pred1* is given in table B.2.

### B.2 Listing of ARLECC

Most of the variable names are identical to the ones used in computer program CNT8SHR. The source code is amply provided with commentary lines. Figure B.1 shows the flow diagram of the program.





```

do ii = 1,nblks
  do jj = 1,nlevs
    read (unit=3) sigmax,sigmin,cycles
    if (sigmax .le. sigmin) stop 9998
    if (sigmax .ge. tyld) stop 9999

    do kk = 1,nint(cycles)

      totcyc = totcyc + 1.
      kmax = corfac*sigmax
      kmin = corfac*sigmin
      dk = kmax - kmin

      if (unretarded) then
        call EFFKMIN(kmin,kmax,fr,kmneff)
        ...kmneff of the current cycle is used
      else
        ...kmneff of the previous cycle is used
      end if
      dkeff = kmax - kmneff
      if ((dkeff .gt. dk) .and. (kk .ne. 1)) dkeff = dk

      if (dkeff .gt. 0.001*dK) then

        dkeff = dlog10(dkeff)

        call TLU(delk,dadn,ndadn,dkeff,da)

        da = 10.**da
        a = a + da

        if (a .ge. w/2) then
          failed = .true.
        else
          corfac = dsqrt(1./dcos(pi*a/w))
          corfac = corfac*dsqrt(pi*a)
          refk = amp*corfac*smax
          if (refk .ge. kc) failed = .true.
        end if
        if (failed) go to 999
      end if

      now check whether current load sigmax is overload...

      if (.not.unretarded) then

        if (sigmax .ge. 0.001) then

          yld = 0.5*pi*sigmax/
            dsqrt(2./dcos(0.5*pi*sigmax/tyld) - 2.)

          if (a .lt. aol+wol) then
            check = kmaxol*dsqrt(1.-(a-aol)/wol)*yld/yldol
          else
            check = 0.
          end if

          if (kmax .gt. check) then
            kmaxol = kmax
            kminol = kmin
            yldol = yld
            aol = a
            wol = (beta/pi)*(kmaxol/yldol)**2.
          end if
        end if

        ...and check whether sigmin is underload...
        (remember that kminol has already been set to kmin in
        case of sigmax being an overload)

        if (kmin .le. kminol + .001*dK) then

          kminol = kmin

          calculate min. eff. stress intensity kmneff...

          call EFFKMIN(kminol,kmaxol,fr,kmneff)
        end if
      end if
    end if
  end if
end if

```

```

        end do

        end do

        hours      = bhrs*ii
        icount     = icount + 1
        ai(icount) = a
        hi(icount) = hours
        write (*, '(lx, f10.2, 2x, f9.6, 2x, e12.4)') hours, a, refk

        rewind (3)

    end do

999 if (failed) then
c   ...specimen has failed
    write (*, '(//lx, a/)') '...specimen has failed'
    icount = icount + 1
    ai(icount) = a
    hi(icount) = bhrs*(totcyc/xcyc)
c   else
    ...nbkls was exceeded
    write (*, '(//lx, a/)') '...maximum number of blocks exceeded'
end if

close (3, status='delete')

c
c   output...
c
44 write (*, '(lx, a, $)') 'Enter the name of your PREDICTION file: '
    read (*, '( a )') ipred
    open (unit=1, file=ipred, status='new', err=44)

    write (1, '(lx, a/)') 'ARL Crack Growth Model...'

    write (1, '(lx, a/)') 'INPUT DATA'

    if (unretarded) then
        write (1, '(lx, a)')
    + 'ALPHA = N.A. (unretarded)'
    else
        write (1, '(lx, a, F7.3)')
    + 'ALPHA =', alpha
    end if
    write (1, '(lx, a, E13.5)') ' Ain =', ain
    write (1, '(lx, a, E13.5)') ' W =', w
    write (1, '(lx, a, E13.5)') ' DLS =', DLS
    write (1, '(lx, a, F7.3/)') ' AMP =', amp

    write (1, '(lx, a, lx, a)') 'Material data: file =', matfil
    write (1, '(lx, a, E11.3)') ' Tyld =', tyld
    write (1, '(lx, a, F7.3)') ' FR =', FR
    write (1, '(lx, a, E11.3/)') ' Kc =', Kc

    write (1, '(lx, a, lx, a)') 'Spectrum data: file =', isfid
    write (1, '(lx, a, 17)') ' Nievs =', nievs
    write (1, '(lx, a, E11.3)') ' Bhrs =', bhrs
    write (1, '(lx, a, E11.3/)') ' Smax =', smax

    write (1, '(//lx, a/)') 'OUTPUT DATA'

    write (1, '(//lx, a)') ' Hours A'
    do ii = 1, icount
        write (1, '(lx, f14.3, f15.6)') hi(ii), ai(ii)
    end do

    close (1)

    stop

    E N D

    subroutine TLU(x, y, n, xval, yval)
    implicit real*8 (a-h, o-z)
    dimension x(50), y(50)

    if (x(n).ge.xval) go to 10
    i = n
    go to 30
10 do 20 i = 1, n

```

## B.6

---

```
      if(x(i).ge.xval) go to 30
20  continue
30  if (i.eq.1) i = 2
      yval = (y(i)-y(i-1))/(x(i)-x(i-1))*(xval-x(i-1))+y(i-1)

      return
      E N D

      subroutine EFFKMIN(kminol,kmaxol,fr,kmneff)
      implicit none
      real*8  kminol,kmaxol,fr,kmneff,SR,U,XR,XFR

      SR = kminol/kmaxol
      U = 0.55 + 0.33*SR + 0.12*SR*SR
      XR = 1.0 - U*(1.- SR)
      XFR = 1.0 - (0.756 - 0.912*FR + 0.156*FR*FR)*(1.- SR)
c     .....U = dkeff/dk is an equation due to Schijve
c     while the equation for XFR has been obtained from McAir.
c     To tune the combination of these equations FR is divided by
c     a factor 1.12 in the main program since Schijve's equation is
c     valid for 2024 and 7075, having a FR of 1.12 approx.

      kmneff = XR*XFR*kmaxol
      if (kmneff .lt. 0.) kmneff = 0.
      if (kmneff .lt. kminol) kmneff = kminol

      return
      E N D
```



ARL Crack Growth Model...

INPUT DATA

ALPHA = .000  
Ain = .20000E-01  
W = .10000E+00  
DLS = .60000E+08  
AMP = 1.000

Material data: file = dadn.dat  
TylD = .457E+09  
FR = .803  
Kc = .490E+08

Spectrum data: file = exampil.seq  
Nlevs = 5  
Bhrs = .100E+03  
Smax = .600E+08

OUTPUT DATA

Hours	A
.000	.020000
100.000	.020908
200.000	.021942
300.000	.023141
400.000	.024566
500.000	.026326
600.000	.028635
700.000	.032063
800.000	.041695
800.007	.056124

Table B.2 Prediction file of first example, named *pred1*.

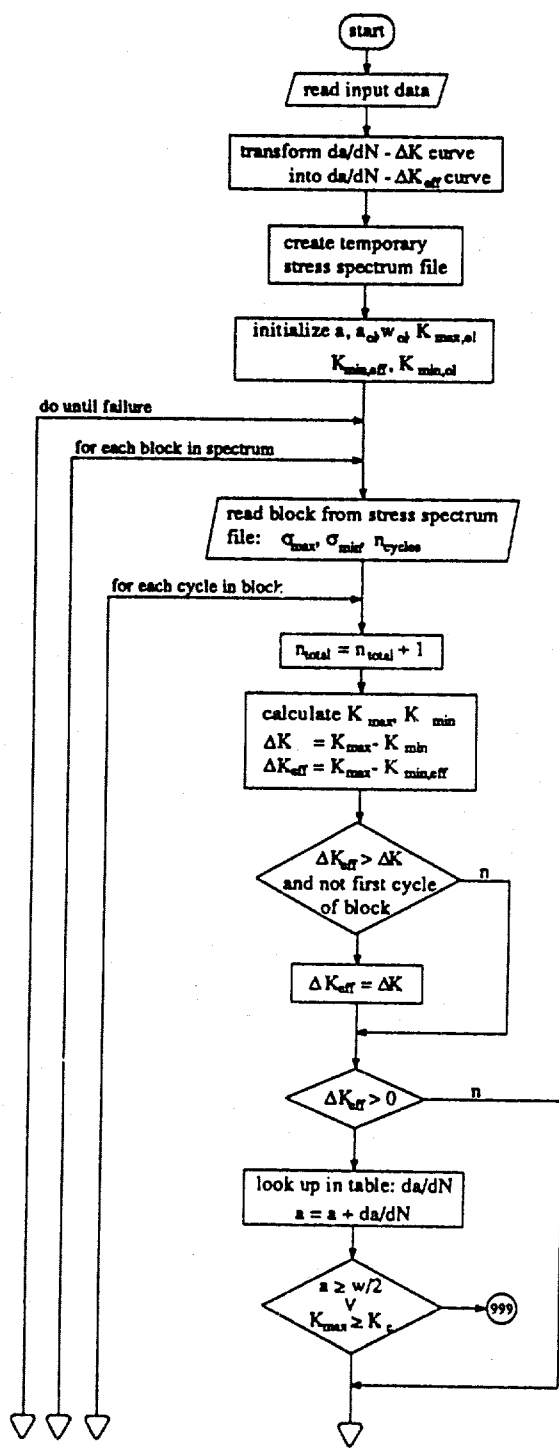


Figure B.1 Flow diagram of computer program ARLECC.

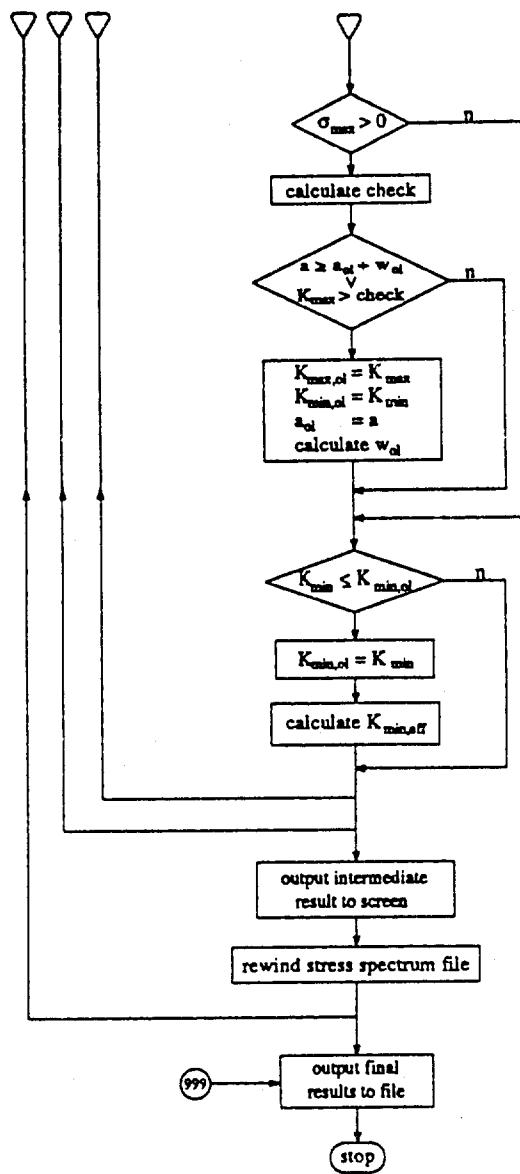


Figure B.1 (continued)

## DISTRIBUTION

### AUSTRALIA

#### Department of Defence

##### Defence Central

Chief Defence Scientist )  
AS, Science Corporate Management ) shared copy  
FAS Science Policy )  
Director, Departmental Publications  
Counsellor, Defence Science, London (Doc Data sheet only)  
Counsellor, Defence Science, Washington (Doc Data sheet only)  
Scientific Adviser, Defence Central  
OIC TRS, Defence Central Library  
Document Exchange Centre, DSTIC (8 copies)  
Defence Intelligence Organisation  
Librarian H Block, Victoria Barracks, Melbourne (Doc Data sheet only)

##### Aeronautical Research Laboratory

Director  
Library  
Chief - Aircraft Structures Division  
Divisional File - Aircraft Structures  
Author: M.J. Bos  
C.K. Rider  
J.G. Sparrow  
J.M. Finney (2 copies)  
G.S. Jost  
D.J. Sherman  
A.D. Graham  
J.M. Grandage  
A.S. Machin  
M. Stimson  
P. Piperias

##### Materials Research Laboratory

Director/Library

##### Defence Science & Technology Organisation - Salisbury

Library

##### Navy Office

Navy Scientific Adviser (3 Copies Doc Data Sheet Only)  
Director of Aircraft Engineering - Navy

##### Army Office

Scientific Adviser - Army (Doc Data Sheet Only)

Air Force Office

Air Force Scientific Adviser  
Engineering Branch Library  
Director General Engineering - Air Force  
HQ Logistics Command (DGELS)

Statutory and State Authorities and Industry

Aero-Space Technologies Australia, Systems Division Librarian  
Ansett Airlines of Australia, Library  
Australian Airlines, Library  
Qantas Airways Limited  
Civil Aviation Authority  
Hawker de Havilland Aust Pty Ltd, Victoria, Library  
Hawker de Havilland Aust Pty Ltd, Bankstown, Library

Universities and Colleges

Adelaide

Professor, Mechanical Engineering

Melbourne

Engineering Library

Monash

Head, Materials Engineering

Newcastle

Library

Professor R. Telfer, Institute of Aviation

Sydney

Engineering Library

NSW

Head, Mechanical Engineering

Library, Australian Defence Force Academy

Tasmania

Engineering Library

Western Australia

Library

Head, Mechanical Engineering

RMIT

Library

Mr M.L. Scott, Aerospace Engineering

**CANADA**

CAARC Coordinator Structures

**NRC**

J.H. Parkin Branch (Aeronautical & Mechanical Engineering Library)

Universities and Colleges

Toronto

Institute for Aerospace Studies

**FRANCE**

ONERA

**INDIA**

CAARC Coordinator Structures

National Aeronautical Laboratory, Information Centre

**INTERNATIONAL COMMITTEE ON AERONAUTICAL FATIGUE**

per Australian ICAF Representative (27 copies)

**ISRAEL**

Technion-Israel Institute of Technology

**JAPAN**

National Research Institute for Metals, Fatigue Testing Div.

**NETHERLANDS**

National Aerospace Laboratory (NLR), Library

**NEW ZEALAND**

Defence Scientific Establishment, Library

Universities

Canterbury

Head, Chemical Engineering

**SINGAPORE**

Director, Defence Materials Organisation

**SWEDEN**

Aeronautical Research Institute, Library

**SWITZERLAND**

F+W (Swiss Federal Aircraft Factory)

## **UNITED KINGDOM**

Defence Research Agency (Aerospace)  
Farnborough, Head Materials Department  
British Library, Document Supply Centre  
CAARC Coordinator, Structures  
British Aerospace  
Kingston-upon-Thames, Library  
Hatfield-Chester Division, Library

### Universities and Colleges

London

Head, Aero Engineering

Manchester

Professor, Applied Mathematics  
Head, Dept of Engineering (Aeronautical)

Cranfield Inst. of Technology

Library

Imperial College

Aeronautics Library

## **UNITED STATES OF AMERICA**

NASA Scientific and Technical Information Facility  
Boeing Commercial Airplanes  
Lockheed California Company  
Lockheed Georgia  
McDonnell Aircraft Company  
Library  
Mr J. Young, F18 Engineering Dept.  
Northrop Corporation, Mr J. Knight, F18 Structural Analysis Org.

### Universities and Colleges

Florida

Aero Engineering Department  
Head, Engineering Sciences

SPARES (10 COPIES)

TOTAL (126 COPIES)

**DOCUMENT CONTROL DATA**PAGE CLASSIFICATION  
UNCLASSIFIED

PRIVACY MARKING

1a. AR NUMBER AR-006-626	1b. ESTABLISHMENT NUMBER ARL-STRUC-R-444	2. DOCUMENT DATE SEPTEMBER 1991	3. TASK NUMBER AIR 89/079
4. TITLE <b>CRITICAL APPRAISAL OF THE McDONNELL DOUGLAS CLOSURE MODEL FOR PREDICTING FATIGUE CRACK GROWTH</b>		5. SECURITY CLASSIFICATION (PLACE APPROPRIATE CLASSIFICATION IN BOXES) (E. SECRET (S), CONF. (C) RESTRICTED (R), UNCLASSIFIED (U)).  <input type="checkbox"/> U <input type="checkbox"/> U <input type="checkbox"/> U DOCUMENT      TITLE      ABSTRACT	6. NO. PAGES  85  7. NO. REFS.  19
8. AUTHOR(S) M.J. BOS		9. DOWNGRADING/DELIMITING INSTRUCTIONS  Not applicable	
10. CORPORATE AUTHOR AND ADDRESS  <b>AERONAUTICAL RESEARCH LABORATORY 506 LORIMER STREET FISHERMENS BEND VIC 3207</b>		11. OFFICE/POSITION RESPONSIBLE FOR: SPONSOR <u>RAAF</u> SECURITY <u>-</u> DOWNGRADING <u>-</u> APPROVAL <u>DARL</u>	
12. SECONDARY DISTRIBUTION (OF THIS DOCUMENT)  Approved for public release  OVERSEAS ENQUIRIES OUTSIDE STATED LIMITATIONS SHOULD BE REFERRED THROUGH DSTIC, ADMINISTRATIVE SERVICES BRANCH, DEPARTMENT OF DEFENCE, ANZAC PARK WEST OFFICES, ACT 2601			
13a. THIS DOCUMENT MAY BE ANNOUNCED IN CATALOGUES AND AWARENESS SERVICES AVAILABLE TO . . .  No limitations			
13b. CITATION FOR OTHER PURPOSES (E. CASUAL ANNOUNCEMENT) MAY BE <input checked="" type="checkbox"/> UNRESTRICTED OR <input type="checkbox"/> AS FOR 13a.			
14. DESCRIPTORS Crack propagation modeling Flight loads Aircraft structures		15. DISCAT SUBJECT CATEGORIES 0103 110601	
16. ABSTRACT <i>The McDonnell Douglas fatigue crack growth model CNTKM8 has been used to predict crack growth in CCT-specimens with through cracks under four different load sequences, including a flight-by-flight sequence, and two stress levels. The predictions were compared against experimental data. The results ranged from fairly good for the more-structured sequences, to rather poor for the more-random sequences. Furthermore, the experimental trend of the structured sequences giving longer crack growth lives than the random sequences was not predicted correctly. An enhanced model was proposed, which was also tested. The predictions of this model were more consistent with the experimental data, and the above-mentioned experimental trend was also predicted correctly.</i>  <i>This report contains a detailed description of both models, including the equations that are relevant for the case of a CCT-specimen with a through crack, and of the tests that they were subjected to.</i>			

PAGE CLASSIFICATION  
UNCLASSIFIED

PRIVACY MARKING

THIS PAGE IS TO BE USED TO RECORD INFORMATION WHICH IS REQUIRED BY THE ESTABLISHMENT FOR ITS OWN USE BUT WHICH WILL NOT BE ADDED TO THE DISTIS DATA UNLESS SPECIFICALLY REQUESTED.

16. ABSTRACT (CONT).

17. IMPRINT

**AERONAUTICAL RESEARCH LABORATORY, MELBOURNE**

18. DOCUMENT SERIES AND NUMBER

Aircraft Structures Report 444

19. COST CODE

25 205A

20. TYPE OF REPORT AND PERIOD COVERED

21. COMPUTER PROGRAMS USED

McAir crack closure CNTKM8  
ARL crack closure ARLECC

22. ESTABLISHMENT FILE REF (S)

23. ADDITIONAL INFORMATION (AS REQUIRED)